



Erasmus Mundus Joint Master degree
Photonics for Security Reliability and Safety



**Politecnico
di Torino**

Master *Photonics for Security Reliability and Safety* (PSRS)



Impact of humidity and temperature on nanowire networks dynamics

Master Thesis Report

Presented by
Khayal Azizli

and defended at

University Jean Monnet

September 4, 2024

Academic Supervisor(s): Prof. Carlo Ricciardi

Host Supervisor(s): Gianluca Milano

Jury Committee: Prof. Dr. Amine NAIT-ALI , Carlo Ricciardi

Acknowledgements

I would like to thank my supervisor, Prof. Carlo Ricciardi, Department of Applied Science and Technology at Polytechnic University of Turin for choosing the topic, advising and supporting me to the expected results from the beginning of the thesis project.

Thanks to Dr. Gianluca Milano also, for providing me access to all related research done by him and Prof. Carlo's team, with access to the great library of previous simulations and experiments done in the area of the topic.

Many thanks to Fabio Michieletti and Davide Pilati, without them electrical measurements done on provided nanowire networks in this research would be impossible since their previous experience and instincts for using these non-linear systems were coming from years of experience.

Last but not least I would like to present my gratitude to my friends, specifically to Udit Pramanik, Anar Imamverdiyev and Agil Shahverdi since they were my biggest inspiration and support in finishing my thesis project. They motivated me in my downtime by pushing me to understand the mentality of never letting go.

Abstract

The use of neural networks in the hardware processing for Artificial Intelligence (AI) has gained significant traction, particularly for solving complex, non-linear, and chaotic problems. A primary objective of this research is to explore the optimal environment for neuromorphic chips, enabling advancements such as increased neural connections, self-healing capabilities, enhanced memory capacity, and energy efficiency. This study focuses on the impact of two critical environmental factors—humidity and temperature cycles—on the dynamic behaviour of Ag-PVP nanowire networks. Through conductance measurements, this research seeks to demonstrate both potentiation and relaxation correlations with external conditions in these networks. The experiments were conducted in a controlled laboratory environment at the Polytechnic University of Turin, utilizing the Keithley 4200-SCS Semiconductor Characterization System for data collection and the Precision Humidity Control System (HCS-2M) for environmental regulation. The findings support the theoretical background and align with previous research, offering generalized insights into the behaviour of these “alive” materials and their potential applications in neuromorphic systems.

Keywords: recurrent neural networks, neuromorphic, environmental impact, relative humidity, temperature cycles, NWs’ dynamics.

Contents

Acknowledgements	i
Abstract	ii
1 Introduction	1
2 Theoretical Foundations of Neuromorphic Systems	4
2.1 Ag-PVP Nanowires and Their Applications	4
2.2 Recurrent Neural Networks, Reservoir Computing and NW applications	7
2.2.1 Reservoir Computing	10
2.2.2 Memory Capacity in Reservoir Computing Systems	11
2.3 Environmental Stability in Nanowire Networks	13
2.3.1 Temperature Effects on Nanowires	13
2.3.2 Relative Humidity Effects on Nanowires	14
2.4 Theoretical Framework for Measurement Techniques	15
2.4.1 Physics Behind Focused Areas of This Work	15
2.4.2 Measurement of Dynamics: Potentiation and Relaxation	16
3 Advances in Nanowire Technology and Applications	18
3.1 Ionic Migration Mechanisms in Resistive Switching	18
3.2 Impact of Environmental Factors on Memristive Behavior	23
3.3 Predictive Modeling of Ion Dynamics in Memristive Devices with MCS .	25
3.3.1 Understanding Monte Carlo Simulations in Ion Dynamics	25
3.3.2 Modeling Ionic Dynamics and Filament Formation in Memristors .	26
3.3.3 Applying Monte Carlo Simulations to Silver Nanowires	28
3.4 ZnO nanowires characteristics under various impact of environment . .	29
3.5 Challenges in Nanowire Fabrication and Application	31

3.6	Future Directions in Neuromorphic Computing	34
4	Experiment design	36
4.1	Ag-PVP Nanowire Networks synthesis and main characteristics	36
4.1.1	Self organizing structure of Ag-PVP NWNs	36
4.1.2	Production of the Ag-PVP nanowires	38
4.2	Experimental Setup	41
4.2.1	Controlling Relative Humidity	41
4.2.2	Piezo-driven probe chamber for various heat applications and humid environments	42
4.2.3	Electrical characterization measurements of the nanowires	43
4.2.4	Experimental steps	43
5	Results	45
5.1	Measurements with continuous V applied	45
5.2	Relative humidity effects on Ag-PVP potentiation	47
5.2.1	G_{\max} vs Time	47
5.2.2	ΔG_0 vs Time	48
5.2.3	G_{\max} vs Relative Humidity	48
5.2.4	ΔG_0 vs Relative Humidity	49
5.2.5	Average ΔG_0 vs Relative Humidity	50
5.3	Temperature effects on Ag-PVP potentiation	51
5.3.1	G_{\max} vs Time across Cycles	51
5.3.2	ΔG_0 vs Time across Cycles	52
5.3.3	G_{\max} vs Temperature across Cycles	52
5.3.4	ΔG_0 vs Temperature across Cycles	53
5.3.5	Average ΔG_0 vs Temperature	54
5.4	Relative humidity effects on new sample with high G	55
6	Conclusion	56
	Non-Plagiarism Statement	69
	Supervisor Approval	70
	Copyright of Figures	71

List of Tables

4.1 Areal mass density of used samples in this work	39
---	----

List of Figures

2.1	a) optical b) SEM c) TEM image d) schematic of coating e) cross-sectional view f) measurement setup of Ag NWs Diaz Alvarez et al. (2019c)	5
2.2	Diagram of Recurrent Neural Networks Salmela et al. (2021)	8
2.3	NW networks Synaptic plasticity. (a) Potentiation followed by network relaxation (b) Spatio-temporal conductance distribution Montano et al. (2022)	17
3.1	Molecular dynamics of Cu-aSi cell between High/low resistance states Onofrio et al. (2015)	20
3.2	Resistive switching I–V characteristics for (a) NiO, (b) Al ₂ O ₃ , (c) TiO ₂ , (d) Nb ₂ O ₅ , (e) MgO, and (f) CoO metal oxide junctions. Figure (f) illustrates the Reset (LRS to HRS) and Set (HRS to LRS) processes Jongmin et al. (2016).	22
3.3	a) Structural similarity of memristor and neural connections b) crossbar array structure Kuncic and Nakayama (2021)	24
3.4	Development of quantum filament Xue et al. (2019a)	27
4.1	Explanation of “reweighting” and “rewiring” of single Ag NW Milano et al. (2022)	37
4.2	Samples with different nanowire densities Milano et al. (2020a)	39
4.3	Diagram of gold deposition on corners	40
4.4	Reformed water droplets on nanowires due to condensation	40
4.5	Experimental Setup	41
4.6	Piezo-driven chamber for many applications MicroprobeSystems (2024a).	42
5.1	Change of G_0 during T,RH,V const	45
5.2	Change of G_0 during T cycle (10-40-10C)	46
5.3	Change of G_{norm} during RH cycle (80-10-80%)	46
5.4	G_{max} vs Time	47
5.5	ΔG_0 vs Time	48
5.6	G_{max} vs Relative Humidity	49
5.7	ΔG_0 vs Relative Humidity	49
5.8	Average G_0 vs Relative Humidity	50

5.9 G_{\max} vs Time	51
5.10 ΔG_0 vs Time	52
5.11 G_{\max} vs Temperature	53
5.12 ΔG_0 vs Temperature	53
5.13 Average ΔG_0 vs Temperature	54
5.14 Average ΔG_0 vs Relative Humidity	55

Abbreviations

AI Artificial intelligence

RNNs Recurrent Neural Networks

LSTM Long Short-Term Memory

MC Memory Capacity

SEM Scanning Electron Microscopy

NWs Nanowires

Ag-PVP Silver-Polyvinylpyrrolidone

NWNs Nanowire Networks

ITO Indium Tin Oxide

HRS High-Resistance State

LRS Low-Resistance State

TCFs Transparent Conductive Films

HCS-2M Precision Humidity Control System

MOSFETs Metal-Oxide-Semiconductor Field-Effect Transistors

MIM Metal-Insulator-Metal

ECM Electrochemical Metallization

PVP Polyvinylpyrrolidone

BPTT Backpropagation Through Time

DANs Directed Acyclic Networks

CVD Chemical Vapor Deposition

NEMS Nanoelectromechanical Systems

MCS Monte Carlo Simulations

PID Proportional-Integral-Derivative

RPM Remote Pulse Measure Unit

MPS Microprobe Stations

Chapter 1

Introduction

The continuous improvement in computational technology has increasingly pushed the boundaries of possibilities in fields such as artificial intelligence (AI), materials science, and nanotechnology. Picked from advancing technologies, neuromorphic computing has earned significant attention for its potential to reshape how we process information, particularly by mimicking the brain's neural architecture and function. Traditional von Neumann architectures face limitations in handling the complex, non-linear tasks that are occurring commonly in modern AI applications. Neuromorphic systems, inspired by the highly interconnected and parallel processing capabilities of the human brain, offer a promising solution.

This thesis work explores the integration of silver-polyvinylpyrrolidone (Ag-PVP) nanowire networks into neuromorphic computing systems, emphasizing their potential to enhance the efficiency and adaptability of these brain-inspired technologies. Ag-PVP nanowires, known for their exceptional electrical conductivity, mechanical flexibility, and stability, exhibit memristive behaviour, which is the key mechanism underlying their neuromorphic properties. This memristive behaviour assists in the development of neuromorphic systems that can potentially surpass the capabilities of biological neural networks.

The major focus of this research is to understand the impact of environmental conditions, particularly humidity and temperature, on the dynamic behaviour of Ag-PVP nanowire networks. These environmental factors play a crucial role in determining the performance and reliability of neuromorphic systems, particularly those based on

nanowire networks. Through a series of experiments conducted in a controlled laboratory environment, this study aims to uncover patterns behind the influence of these environmental conditions on the electrical properties and overall functionality of Ag-PVP NWNs.

Further investigation of the potential of these nanowires to build the foundation of next-generation neuromorphic chips, which are expected to drive significant advancements in AI hardware. The ability of Ag-PVP nanowires to undergo potentiation and relaxation reminding signal processing by biological synapses, gives them the right to be chosen as ideal candidates for neuromorphic systems that will require high adaptability and energy efficiency.

The experiments presented in this work were designed with careful consideration and executed at the Polytechnic University of Turin, employing pieces of equipment such as the Keithley 4200-SCS Semiconductor Characterization System and the Precision Humidity Control System (HCS-2M). These tools enabled precise control over the environmental conditions, ensuring the reliability and accuracy of the collected data.

The insights from this research contribute to the theoretical understanding of nanowire dynamics under varying environmental conditions and also offer practical insights into their application in neuromorphic computing. By integrating Ag-PVP nanowires into neuromorphic systems, this thesis aims to put light on the development of more scalable, and tunable hardware in decided environments, ultimately contributing to the wider application of neuromorphic engineering.

Thesis outline

This thesis is structured to explore the different roles of Ag-PVP nanowire networks in neuromorphic computing, pointing out their potential to be used as brain-inspired hardware.

Chapter 2 presents an in-depth review of Ag-PVP nanowires, exploring their creation, unique characteristics, and a range of practical uses. It also delves into the role of Recurrent Neural Networks (RNNs) in neuromorphic computing, drawing connections between the behaviour of biological neural networks and that of synthetic nanowire networks.

In Chapter 3, the discussion shifts to the latest developments in nanowire technology, particularly focusing on how ionic migration influences resistive switching, how envi-

ronmental conditions affect memristive behaviour, and how Monte Carlo simulations can be used for predictive modelling in this context.

Chapter 4 dives into the experimental design, outlining the synthesis of Ag-PVP nanowire networks and the methods used to study their behaviour under varying environmental conditions. This chapter also discusses the experimental setup, including the tools and techniques used for electrical characterization and environmental control.

In Chapter 5, the results of the experiments are presented, focusing on the effects of temperature and humidity on the potentiation and relaxation dynamics of Ag-PVP nanowires. The chapter offers a detailed analysis of the data, supported by graphs and tables, to provide a comprehensive understanding of how these nanowires perform under different conditions.

Chapter 6 provides the conclusions of the thesis work, summarizing the key findings and stating final observations on the effects of humidity and temperature over nanowire networks, given by results.

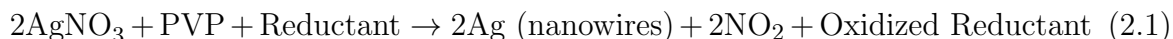
By going through these topics, the thesis aims to contribute to the broadening of vision in the knowledge of neuromorphic computing.

Chapter 2

Theoretical Foundations of Neuromorphic Systems

2.1 Ag-PVP Nanowires and Their Applications

Silver nanowires stabilized with polyvinylpyrrolidone (PVP), commonly referred to as Ag-PVP nanowires, have become increasingly significant in various technological fields due to their unique combination of properties. These nanowires are typically produced through a chemical reduction process, where silver nitrate (AgNO_3) is reduced in the presence of PVP. The general reaction for this synthesis can be represented as:



PVP plays a dual role in this process: it acts as a stabilizer that prevents the silver particles from aggregating and as a growth-directing agent that ensures the formation of nanowires with a high aspect ratio. As the schematic view of the coating presented in Figure 2.1e, the nanowires have a much greater length compared to their diameter, which is usually between 20 and 100 nanometers, while their length can extend to several micrometres [Bao et al. \(2019\)](#).

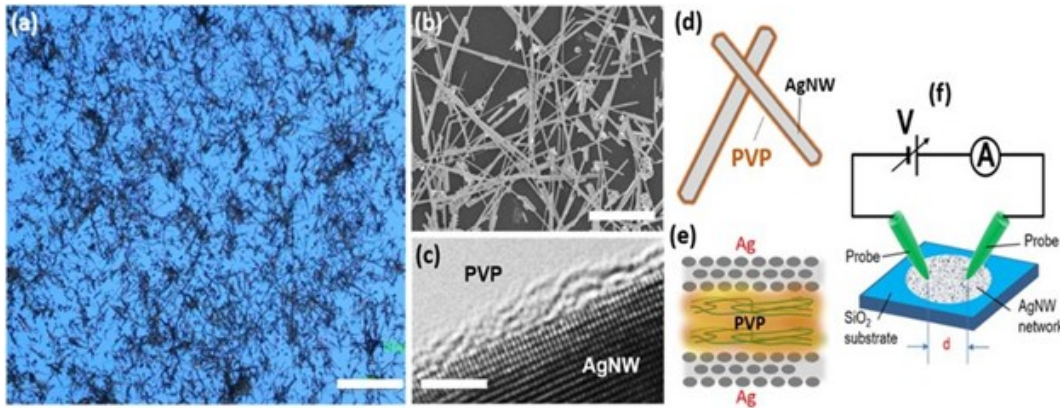


Figure 2.1: a) optical b) SEM c) TEM image d) schematic of coating e) cross-sectional view f) measurement setup of Ag NWs [Diaz Alvarez et al. \(2019c\)](#)

One of the most prominent applications of Ag-PVP nanowires is in the development of transparent conductive films (TCFs). TCFs are critical components in a variety of modern devices, including touch screens, flexible displays, and solar cells. The structure of Ag-PVP nanowires allows them to form networks that combine high electrical conductivity with excellent optical transparency. The relationship between sheet resistance (R_s), resistivity (ρ), and thickness (t) of the nanowire network is given by the equation:

$$R_s = \frac{\rho}{t} \quad (2.2)$$

Research has shown that these films can achieve sheet resistances as low as 10 ohms per square while maintaining transparency levels above 90%, making them a competitive alternative to the more commonly used indium tin oxide (ITO) films. ITO is known for its brittleness and higher cost, which makes Ag-PVP nanowires an attractive option for applications requiring both flexibility and transparency [Kim et al. \(2001\)](#).

The flexibility of Ag-PVP nanowires is particularly beneficial in the realm of wearable electronics. These nanowires can be embedded into flexible substrates to create circuits that maintain their electrical conductivity even when subjected to mechanical stress such as bending, stretching, or folding. This makes them ideal for use in devices like bendable displays, wearable sensors, and electronic textiles. The ability of Ag-PVP nanowires to endure repeated mechanical deformation without significant loss in performance is due to their high aspect ratio and the strong adhesion between the nanowires and the substrate material [Hu et al. \(2010\)](#).

In addition to their use in flexible electronics, Ag-PVP nanowires are also highly effective in sensing applications. Their large surface area and excellent electrical properties make them highly sensitive to changes in their environment, such as the presence of gases or biological molecules. For example, sensors made from Ag-PVP nanowires can detect low concentrations of ammonia or hydrogen gas by measuring changes in the nanowires' electrical resistance when these gases are absorbed onto their surface. Similarly, in biosensing applications, these nanowires can detect biomolecules like glucose with high sensitivity, making them valuable for medical diagnostics and environmental monitoring [Bao et al. \(2019\)](#).

Another important application of Ag-PVP nanowires is in antimicrobial treatments. Silver has long been recognized for its antibacterial and antiviral properties, and these effects are even more pronounced when silver is structured at the nanoscale. The large surface area of Ag-PVP nanowires enhances their interaction with microbial cells, making them more effective at killing bacteria and viruses. This makes Ag-PVP nanowires suitable for use in medical devices, surgical instruments, and wound dressings, where they can provide long-lasting antimicrobial protection without causing cytotoxic effects to human cells [Hu et al. \(2010\)](#).

Ag-PVP NWs have emerged as a promising material for neuromorphic computing due to their exceptional electrical conductivity and stability for creating dynamic and adaptive neuromorphic circuits. The PVP coating on these nanowires not only stabilizes the silver core but also provides a tunable interface that can be engineered to interact with the surrounding environment in controlled ways, developing the network's adaptability.

In neuromorphic systems, Ag-PVP nanowires can serve as the fundamental building blocks of synaptic connections, which are crucial for signal transmission and processing within the network. Their ability allows them to effectively mimic the plasticity of biological synapses. This plasticity is central to learning and memory functions in neuromorphic systems, where the strength of connections between nodes (or neurons) can be adjusted based on experience or training data.

The high aspect ratio of Ag-PVP nanowires ensures efficient electron transport, even in densely packed networks, which is crucial for the high-speed processing required in neuromorphic applications. While going further during this work there is a more detailed review of neuromorphic applications that will be extensively deepened in the

following sections.

After revising general applications it can be told that Ag-PVP nanowires are an adaptable and promising nanomaterial within a wide range of applications. Their unique combination of high conductivity, optical transparency, mechanical flexibility, and antimicrobial properties makes them suitable for use in transparent conductive films, flexible electronics, sensors, and biomedical devices. As research in this area continues to advance, Ag-PVP nanowires are likely to play a crucial role in the development of next-generation technologies [Kim et al. \(2001\)](#).

2.2 Recurrent Neural Networks, Reservoir Computing and NW applications

Recurrent Neural Networks (RNNs) are a specialized type of neural network that excels at processing sequential data. Unlike traditional feedforward neural networks that process inputs independently of each other, RNNs are designed to retain information over time. This is achieved through the use of feedback loops that allow information to persist within the network. This capability makes RNNs particularly effective for tasks where the order of inputs is essential, such as language processing or time series forecasting [Hochreiter and Schmidhuber \(1997\)](#) [Elman \(1990\)](#).

At the core of an RNN is the recurrent neuron. What sets this neuron apart is its ability to take input not only from the current data point but also from the previous time steps. This means the network can maintain a form of memory, which is vital for understanding sequences over time. Mathematically, the hidden state h_t at time step t is calculated using the equation [Heaton \(2017\)](#) [Cho et al. \(2014b\)](#):

$$h_t = f(W_h h_{t-1} + W_x x_t + b) \quad (2.3)$$

In this equation:

- W_h and W_x represent the weight matrices,
- x_t is the current input,
- h_{t-1} is the hidden state from the previous time step,
- b is the bias term, and

- f is an activation function like tanh or ReLU, which introduces non-linearity to the model.

However, RNNs are not without their challenges. One of the most significant issues is the vanishing gradient problem. This occurs when the gradients used in backpropagation through time (BPTT) become very small, making it difficult for the network to learn dependencies that span many time steps. This limitation is particularly problematic for tasks that require long-term memory, as the network struggles to retain relevant information from earlier in the sequence [Bengio et al. \(1994\)](#) [Pascanu et al. \(2012\)](#).

To overcome these limitations, more advanced versions of RNNs have been developed, such as Long Short-Term Memory (LSTM) networks. LSTMs incorporate a sophisticated memory system that uses gates to control the flow of information. These gates—input, forget, and output—decide which information should be kept, discarded, or outputted at each time step. The LSTM architecture includes a cell state, denoted as C_t , which acts like a conveyor belt, carrying relevant information across time steps with minimal changes, thus enabling the network to remember important details over long sequences [Gers et al. \(2000\)](#) [Cho et al. \(2014a\)](#).

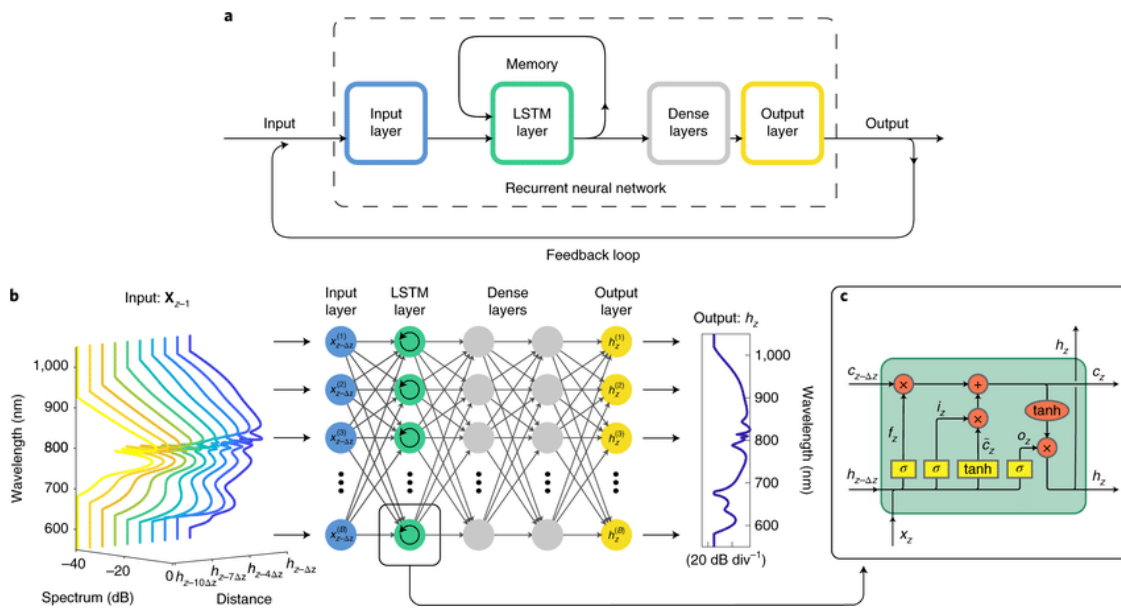


Figure 2.2: Diagram of Recurrent Neural Networks [Salmela et al. \(2021\)](#)

Figure 2.2 provided earlier offers a visual representation of an RNN architecture that includes an LSTM layer. How data flows through the network, starting from the input

layer, passing through the LSTM layer, and then through dense layers before producing output is successfully highlighted by diagrams. The LSTM layer is particularly noteworthy because it uses its memory capabilities to retain crucial information over time, which is then processed further in the dense layers to produce the final output.

Moreover, the graph also details the internal workings of an LSTM cell. Within each LSTM cell, the data is carefully managed by various gates [Gers et al. \(2000\)](#):

- **Input Gate (i_t):** Determines how much of the new information will be added to the cell state.
- **Forget Gate (f_t):** Decides what portion of the existing cell state should be forgotten or retained.
- **Output Gate (o_t):** Controls what part of the cell state will be used to produce the output.

This gating mechanism allows the LSTM to selectively retain or discard information, ensuring that only the most relevant data influences the output. For example, in time series prediction, an LSTM can remember important trends and patterns from earlier in the sequence while ignoring irrelevant fluctuations.

Another variant of RNNs is the Gated Recurrent Unit (GRU), which simplifies the LSTM by combining some of the gates into a single update gate, reducing the computational complexity while still addressing the vanishing gradient problem.

Despite these advancements, RNNs, particularly deep RNNs with multiple layers, remain computationally intensive. As the network depth increases, so does its capacity to model complex temporal dependencies. However, this also results in a higher computational load and more challenging training processes. Researchers continue to explore ways to optimize RNNs, balancing the depth and efficiency of the network while mitigating issues like the vanishing gradient [Sutskever et al. \(2014\)](#).

Recurrent Neural Networks, especially with enhancements like LSTM and GRU layers, are powerful tools for handling sequential data. The feedback loops and memory mechanisms they employ allow them to excel in tasks requiring an understanding of the temporal dynamics within data. As computational techniques and architectures continue to evolve, the capabilities and applications of RNNs will undoubtedly expand, offering even more sophisticated solutions for processing sequential data [Graves \(2013\)](#).

2.2.1 Reservoir Computing

The reservoir computing (RC) method is built on transforming input signals into a high-dimensional feature space by utilizing a reservoir, which is essentially a complex network of interconnected nonlinear elements. The main advantage of RC lies in its approach: only the readout layer responsible for interpreting the state of the reservoir requires training. [Schrauwen et al. \(2007\)](#)

The main inspiration for building principles is taken from recurrent neural networks (RNNs) but with a significant simplification. Unlike traditional RNNs, RC takes advantage of the intrinsic dynamics of a reservoir. This reservoir is a large, fixed network of interconnected units that project input data into a high-dimensional space, making the data linearly separable. By doing so simple linear methods can effectively classify or predict outcomes with high precision.

Memristive nanowire networks are ideally suited for reservoir computing because they naturally exhibit complex, nonlinear dynamics and memory capacity characteristics important for processing temporal information. Ag NWNs which consist of nanowires coated with materials such as PVP, function as memristive elements at their junctions. When a voltage is applied, these junctions alter their resistance states, enabling the network to “remember” past inputs for tasks such as time series prediction. Each junction between the nanowires with its resistance modifiable by an electric field, allows the network to function as a physical reservoir within an RC system.

Characteristics of the nanowire network include fading memory properties, where the impact of past inputs diminishes gradually over time. This behaviour is similar to short-term memory in biological neural systems, dynamic change caused by applied voltage to different junctions enables the network to map input signals into a complex, high-dimensional feature space.

Time Series Prediction: One of the main applications of RC using memristive nanowire networks is predicting chaotic time series, like the Mackey-Glass series. By feeding the time series into the network, its complex dynamics allow for capturing underlying patterns, which can then be predicted accurately using a straightforward linear readout. [Milano et al. \(2022\)](#)

Pattern Recognition: Another significant application is recognizing spatio-temporal patterns. For example, the memristive network can process inputs that represent various patterns, such as handwritten digits from the dataset. The reservoir maps these

inputs into distinct states, which can be easily classified by a linear readout layer. [Appeltant et al. \(2011\)](#)

The efficiency of RC stands out when managing multiple tasks simultaneously by associating different readout layers with the same reservoir. This multitasking ability is worth considering advantage over traditional computing methods, creating possible applications for a broad range of areas from speech recognition to sensor data processing in robotics.

2.2.2 Memory Capacity in Reservoir Computing Systems

Memory capacity (MC) is a vital aspect of reservoir computing (RC) systems, which determines how effectively the system can store and retrieve previously input information. In RC systems, input data is projected into a high-dimensional space using a dynamic reservoir, usually consisting of a recurrent neural network or another form of a nonlinear dynamic system. The MC of an RC system is crucial for its performance in tasks like time-series prediction, pattern recognition, and other activities that require access to past data.

In simpler linear RC models, MC is often linked to the characteristics of the reservoir network. However, when dealing with more intricate reservoir networks, such as those structured with Directed Acyclic Networks (DANs), the conventional theoretical predictions for MC become inadequate. Therefore, analyzing MC in these contexts requires taking into account the unique structural features of the reservoir network.

Theoretical Analysis of Memory Capacity

In a standard reservoir computing system, MC can be conceptualized as the system's ability to recreate a delayed version of its input. For instance, consider an input at time t denoted as $x(t)$. If the reservoir is capable of reconstructing the delayed input $x(t - \tau)$ for $\tau = 1, 2, \dots, S$, then a readout matrix $W_{\text{out}}^{(\tau)}$ must exist, satisfying the equation:

$$x(t - \tau) = W_{\text{out}}^{(\tau)} R(t), \quad \tau = 1, \dots, S.$$

In this scenario, $R(t)$ signifies the reservoir state at time t . The present input $x(t)$ can also be retrieved from the reservoir state:

$$x(t) = W_{\text{out}}^{(0)} R(t).$$

Within this framework, if $\tau = P$, the MC is theoretically capped at $P - 1$, where P represents the longest path length within the reservoir’s DAN. [Jaeger \(2002\)](#)

This theoretical ceiling implies that the MC’s upper limit is determined by the reservoir network’s structural properties, particularly its capacity to remember past inputs over time without losing information.

This theoretical constraint on MC is mathematically expressed as:

$$\text{MC}_{\max} = P - 1.$$

Experimental Validation and Influencing Factors of Memory Capacity

To verify the theoretical upper limit of MC, numerical experiments are carried out using DANs with varying longest path lengths P [Farka et al. \(2016\)](#). In these trials, MC is assessed by examining the system’s ability to recall delayed inputs $x(t - \tau)$ for $\tau = 1, \dots, 30$. The results from these experiments demonstrate that the maximum MC observed across 100 repeated tests does not surpass the theoretical limit of $P - 1$.

Moreover, the experiments [Han et al. \(2021\)](#) reveal that MC is influenced by factors beyond the longest path length P . These factors include:

- *Reservoir Network Size (N):* The results indicate that MC achieves an optimal level regardless of the network size when P is relatively small. However, for larger P values, MC tends to grow with the network size.
- *Network Scaling Hyperparameter (c):* The experiments show that MC fluctuates with changes in the network scaling parameter c . Initially, MC improves as c increases, but it eventually declines as c continues to rise.
- *Input Scaling Hyperparameter (ξ):* Similar to network scaling, input scaling also impacts MC. Larger input scaling values generally reduce MC, suggesting a trade-off between input magnitude and the system’s memory retention capabilities.
- *Reservoir Network Density (D):* The density of the reservoir network, which is defined by the proportion of active connections within the network, also affects MC. Higher network density typically enhances MC, as a denser network is better equipped to maintain information over time.

2.3 Environmental Stability in Nanowire Networks

Nanowires, attributable to their elevated surface area-to-volume ratio and distinctive electronic, optical, and mechanical characteristics, have been extensively examined under a variety of environmental conditions to comprehend how elements such as temperature and relative humidity influence their behavior and prospective applications. The response of nanowires to these environmental parameters is paramount for their implementation in sensors, electronics, and other apparatus that function in heterogeneous and occasionally extreme environments.

2.3.1 Temperature Effects on Nanowires

Temperature constitutes a vital variable that affects the properties and efficacy of nanowire materials. Investigations have indicated that fluctuations in temperature can influence the electrical conductivity, mechanical resilience, and phase stability of nanowires. Temperature has an undeniable effect on the memristive behaviour of devices which are further explained since it's one of the main points of the thesis work.

Electrical Conductivity

Analyses on metallic nanowires, such as silver (Ag) and gold (Au), have substantiated that their electrical conductivity diminishes with increasing temperature due to intensified electron-phonon scattering. For instance, silver nanowires manifest a decline in conductivity as temperature ascends, which is a critical consideration for their application in flexible electronics that may operate under varying thermal conditions [Tarasevich et al. \(2022\)](#).

Phase Transitions

Semiconductor nanowires, such as those fabricated from zinc oxide (ZnO) and gallium nitride (GaN), have been scrutinized for their phase stability under disparate temperatures. ZnO nanowires, for example, preserve their wurtzite crystal structure up to relatively elevated temperatures, yet phase transitions or morphological alterations can transpire at extreme temperatures, influencing their electronic and optical properties [Awad et al. \(2014\)](#). GaN nanowires also demonstrate significant thermal stability, rendering them suitable for high-temperature applications such as high-power electronics and optoelectronics.

Mechanical Properties

The mechanical resilience and flexibility of nanowires may also exhibit temperature dependence. Investigations on silicon (Si) nanowires have revealed that their fracture toughness diminishes with increasing temperature, which could restrict their utilization in high-temperature environments [Wang et al. \(2017\)](#). This is particularly significant for nanowires employed in nanoelectromechanical systems (NEMS) and other devices where mechanical integrity is imperative.

2.3.2 Relative Humidity Effects on Nanowires

Relative humidity (RH) represents an additional environmental variable that can substantially influence the characteristics of nanowire materials, particularly those employed in sensing applications. Similar to temperature change in relative humidity causes a change in the memristive behaviour of devices which is further explained since it's the second main focus of this work.

Sensing Applications

Nanowires composed of substances such as tin oxide (SnO_2) and indium oxide (In_2O_3) have been extensively examined for their sensitivity to fluctuations in humidity. These metal oxide nanowires are frequently utilized in humidity sensors due to their electrical resistance alterations in response to water vapor adsorption on their surfaces. For instance, SnO_2 nanowires demonstrate an elevation in resistance as relative humidity escalates, attributable to the generation of a water layer on their surface that obstructs electron mobility [Kuang et al. \(2007\)](#). This attribute is harnessed in environmental surveillance and intelligent home devices for precise humidity detection.

Surface Chemistry

The interplay between nanowires and water molecules is also pivotal for comprehending their efficacy under varying humidity circumstances. For example, investigations of ZnO nanowires have revealed that surface hydroxylation (the generation of OH groups on the surface) may transpire in high-humidity settings, modifying the surface charge and potentially influencing the electronic and photonic characteristics of the nanowires. This phenomenon is particularly pertinent in applications such as gas sensors and photocatalysis. [Zhang et al. \(2012\)](#)

2.4 Theoretical Framework for Measurement Techniques

2.4.1 Physics Behind Focused Areas of This Work

The behaviour of Ag-PVP nanowires under varying environmental conditions is central to this research, particularly in their application within neuromorphic computing systems. Neuromorphic computing seeks to emulate the functionality of the human brain, where synaptic connections are represented by the conductance properties of nanowire networks. To achieve this, it is crucial to understand how the conductance of Ag-PVP nanowires responds to external stimuli such as voltage pulses, temperature variations, and humidity.

Conductance (G), simply put measures a material's conductance ability of electric current. It is mathematically defined as the inverse of resistance (R), given by the relation $G = \frac{1}{R}$. In the context of this research, the conductance of Ag-PVP nanowires is monitored as a function of time, particularly under the influence of varying environmental conditions.

A key parameter in analyzing these dynamics is the time constant (τ). The time constant is a measure of the response speed of the nanowires to an external voltage pulse. In capacitive systems, (τ) is the time required for the system, to reach approximately 2/3 of its maximum magnitude following a step change in voltage. The time constant can be expressed as [Septiningrum et al. \(2019\)](#):

$$\tau = RC$$

where R is the resistance and C is the capacitance of the system. In the context of neuromorphic computing, a shorter time constant indicates a faster response, which is crucial for applications requiring rapid signal processing and memory retention [Diaz Alvarez et al. \(2019b\)](#).

Voltage pulse signals are used to characterize the conductance dynamics of nanowires. By applying a controlled series of voltage pulses, the research investigates how the conductance changes over time. The conductance response to these pulses provides insight into the potentiation (increase in conductance) and relaxation (decrease in conductance) behaviors of the nanowires [Montano et al. \(2022\)](#). This understanding is pivotal for optimizing these materials for use in next-generation neuromorphic computing systems.

2.4.2 Measurement of Dynamics: Potentiation and Relaxation

The dynamic processes of potentiation and relaxation are essential in understanding the functionality of Ag-PVP nanowires within neuromorphic systems. These processes mirror the synaptic strengthening and weakening observed in biological neurons.

Potentiation refers to the process by which the conductance of the nanowire increases in response to the application of voltage. This increase in conductance can be attributed to mechanisms such as ion migration within the nanowire or the formation of conductive filaments, which enhance the connectivity between nanowires [Septiningrum et al. \(2019\)](#). This behaviour is critical in neuromorphic systems, where synaptic connections need to be strengthened in response to learning stimuli.

The mathematical representation of potentiation can be linked to the change in conductance (ΔG) over time, which can be modelled as:

$$\Delta G(t) = G_0 \left(1 - e^{-\frac{t}{\tau}}\right)$$

where G_0 is the initial conductance and τ is the time constant.

Relaxation, on the other hand, occurs when the external stimulus (voltage pulse) is removed, leading to a decrease in conductance over time. This decrease is a result of the dissipation of charge carriers, the reversion of ion migration, or the reconfiguration of the nanowire network. Relaxation is critical for the reset functionality in neuromorphic systems, allowing the system to return to its baseline state after processing a signal. Also for the elaboration of temporal signals since the effect of a pulse at $t+1$ is dependent on how much the network relaxed from the end of the previous pulse.

The relaxation process can be described by an exponential decay model:

$$G(t) = G_{\max} e^{-\frac{t}{\tau}}$$

where G_{\max} is the maximum conductance achieved during potentiation.

In Fig. 2.3.a 4 V input voltage pulse was applied, with conductance measured and modeled accordingly. The potentiation phase lasted for 10 seconds, followed by a 70-second relaxation at a reading voltage of 50 mV. Meanwhile part b. explains spatio-temporal changes in conductance across the network are depicted, highlighting the formation and eventual breakdown of conductive pathways. The red colour of the edges corresponds to their conductance, blue represents the voltage at each node, arrows

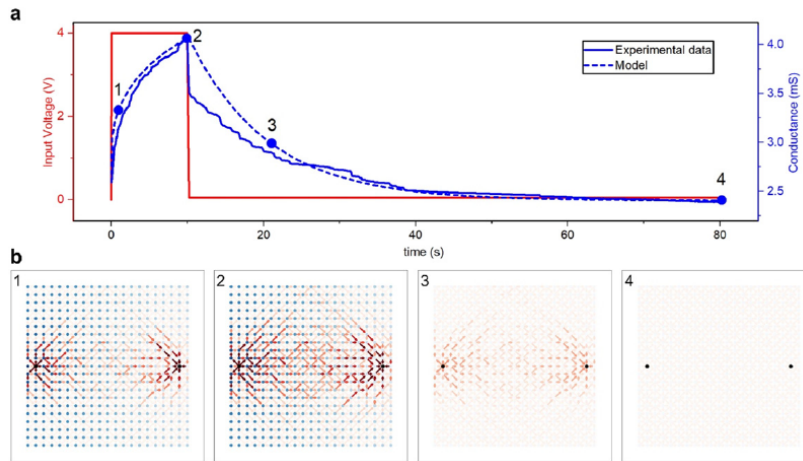


Figure 2.3: NW networks Synaptic plasticity. (a) Potentiation followed by network relaxation (b) Spatio-temporal conductance distribution [Montano et al. \(2022\)](#)

show the direction of current flow, and black nodes denote the input terminals. The left electrode was subject to a bias, with the right electrode grounded. [Montano et al. \(2022\)](#)

To measure these dynamics, a series of voltage pulses are applied to the nanowire network, and the conductance is monitored in real time. The resulting conductance-time curves provide valuable information about the speed, stability, and reversibility of the potentiation and relaxation processes. These measurements are essential for evaluating the suitability of Ag-PVP nanowire networks for use in neuromorphic applications, where fast and reliable switching between different conductance states is required.

Chapter 3

Advances in Nanowire Technology and Applications

3.1 Ionic Migration Mechanisms in Resistive Switching

Resistive switching memory is a foundational stone of non-volatile memory technology, driven by the unique behaviours of nanoscale materials under electrical bias. These mechanisms, particularly ionic migration and electrochemical metallization, are essential to understanding how memristive devices operate, especially in dynamic environments where factors like temperature and humidity can significantly alter device performance. Resistive switching memory has been observed across various functional materials, including phase-change memory, ferroelectric and ferromagnetic materials. The resistance change in these materials can be attributed to nanoscale geometric confinement, which modifies the material's band structure and associated tunnel barrier. However, more commonly, the large surface-area-to-volume ratio in these nanoscale systems enhances bias-catalyzed redox reactions that couple electronic and ionic transport [Waser et al. \(2009\)](#); [Yang et al. \(2013\)](#).

In electrolytic materials, which are electrically insulating and ionically conducting, resistive switching is primarily driven by the formation and dissolution of conductive filaments within a metal-insulator-metal (MIM) junction. This process mimics biological synaptic dynamics, where neurotransmitter molecules regulate synaptic strength, analogous to how ionic migration modulates the resistive state in memristors.

Ionic dynamics play a crucial role in the formation and dissolution of conductive filaments, which are responsible for the switching between high-resistance (HRS) and low-resistance states (LRS) in memristive devices.

Ion Migration: Under an applied electric field, metal cations or oxygen vacancies migrate through the active layer. For example, in metal-core nanowire systems, metal cations like Ag migrate across the MIM junction, forming a metallic filament at the cathode nanowire [Song and Yang \(2022\)](#). This process changes the device from HRS to LRS as the filament provides a low-resistance path for electron flow.

Ion Diffusion: In addition to migration, ions can also diffuse due to concentration gradients. This diffusion is slower but contributes to the long-term stability of the resistive states by influencing the retention time of the memristor's state once the external field is removed.

Resistive switching memory devices can be categorized based on their working principles into three primary types: Valence Change Memories (VCM), Thermochemical Memories (TCM) and Electrochemical Metallization (ECM) memories. Each of these types leverages distinct mechanisms to form and dissolve conductive pathways within the memory material, which are crucial for data storage and retrieval.

Valence Change Memories (VCM): VCMs operate by altering the distribution of oxygen vacancies or anions within a dielectric material. The resistance change is driven by modulating the valence state of transition metal ions, which affects the material's conductivity. The creation and annihilation of oxygen vacancies within the dielectric layer lead to the formation or dissolution of conductive paths, corresponding to the low and high resistance states.

Thermochemical Memories (TCM): TCMs depend on localized heating to induce a chemical reaction within the material, which changes its resistance. Typically, the heat generated by an applied voltage triggers a redox reaction that alters the material's phase or composition, forming a conductive path. This change is reversible; as the material cools, the reaction can reverse, returning the system to its high-resistance state.

Electrochemical Metallization (ECM): ECM is a process where metal cations from an anode nanowire migrate across the junction and are reduced at the cathode, forming a conductive filament. This process is reversible; applying a reverse bias dissolves the filament as the metal atoms ionize and migrate back towards the anode, reinstating the high-resistance state. The atomistic simulations depicted in Figure 3.1 show the

formation and rupture of these filaments within a Cu-aSi cell, which is critical for understanding the switching dynamics at a molecular level.

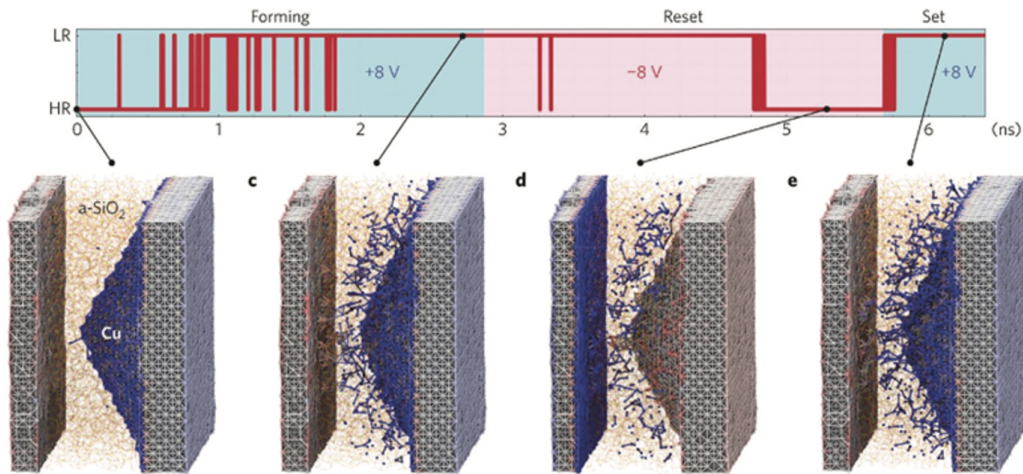


Figure 3.1: Molecular dynamics of Cu-aSi cell between High/Low resistance states [Onofrio et al. \(2015\)](#)

Molecular dynamics simulations illustrate the metallization process during forming, reset, and set cycles in a Cu-aSi cell, showing the transition between high resistance (HR) and low resistance (LR) states. This figure emphasizes how the applied voltage influences the switching process by driving the electrochemical reactions that create or dissolve the conductive pathways [Onofrio et al. \(2015\)](#).

Resistive switching, a key principle in the operation of many non-volatile memory devices, particularly memristors, is heavily influenced by the movement of ions within the device's active layer. This process, known as ionic migration, involves the drift and diffusion of charged particles—usually oxygen vacancies, metal cations, or anions—under the effect of an electric field. Ionic migration is crucial for the creation and breakdown of conductive filaments or the adjustment of defect states, which are responsible for switching the device between its high and low resistive states. Understanding how ionic migration works is essential for optimizing these resistive switching devices, especially for applications in data storage, neuromorphic computing, and reconfigurable logic systems. These mechanisms are generally classified into unipolar and bipolar switching, depending on the nature of the applied voltage and the material's response. In our further cases, we are interested in bipolar switching since voltage polarity is reversed.

Bipolar switching requires reversing the voltage polarity to switch between HRS

and LRS. This type of switching is common in systems where ionic movement and electrochemical reactions are highly dependent on the applied voltage's polarity. For instance, in Ag-based systems, a positive bias drives Ag⁺ ions towards the cathode, forming a filament, while a negative bias dissolves the filament, returning the device to HRS.

The transition from high-resistance state (HRS) to low-resistance state (LRS) is typically associated with the formation of a conductive filament, often composed of reduced metal ions or oxygen-deficient regions within a metal oxide. These oxygen vacancies act as mobile charge carriers that respond to an applied electric field, forming a conductive filament that connects the electrodes. This process changes the device from a high-resistance state (HRS) to a low-resistance state (LRS) [Waser and Aono \(2007\)](#). When the voltage polarity is reversed, the conductive filament dissolves as the oxygen vacancies return to their original positions, reinstating the high-resistance state. This continuous cycle of ion migration is at the heart of resistive switching, making the non-volatile memory effect in memristive devices possible.

In addition to oxygen vacancy migration, metal ion migration plays a significant role in resistive switching, especially in silver (Ag) or copper (Cu)-based resistive random-access memory (ReRAM) devices. When a positive voltage is applied, these metal ions are reduced and deposited in the dielectric, forming a metallic filament that lowers the device's resistance. When the filament dissolves through the reverse migration of metal ions, the device returns to its high-resistance state [Yang et al. \(2013\)](#).

Fig.3.2 shows the resistive switching I-V characteristics for various metal-oxide-metal systems. The I-V curves exhibit hysteresis loops that are indicative of the resistive switching behaviour. The current in this graph is in logarithmic scale and the current changes sign from set to reset. The LRS and HRS I-V properties are portrayed by the blue and red curves, correspondingly. These loops provide insights into the energy required for switching and the stability of the memristive states under different environmental conditions.

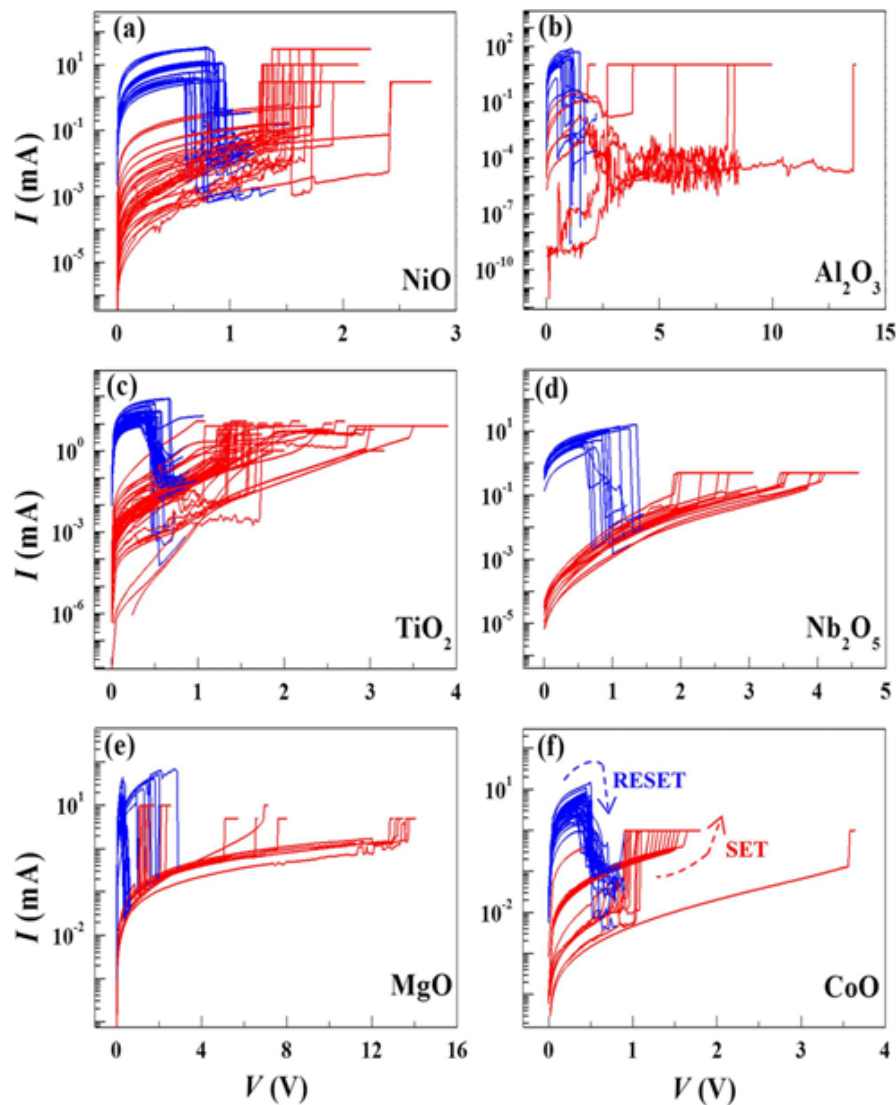


Figure 3.2: Resistive switching I–V characteristics for (a) NiO, (b) Al_2O_3 , (c) TiO_2 , (d) Nb_2O_5 , (e) MgO, and (f) CoO metal oxide junctions. Figure (f) illustrates the Reset (LRS to HRS) and Set (HRS to LRS) processes [Jongmin et al. \(2016\)](#).

The speed and behaviour of ionic migration are affected by several factors, including the strength of the electric field, temperature, and the material composition of the device. For example, stronger electric fields tend to accelerate the migration of ions, resulting in quicker switching times. Similarly, higher temperatures generally increase the mobility of ions, speeding up their movement within the active layer [Sawa \(2008\)](#). However, if the migration of ions is too rapid or extensive, due to high electric fields or sustained elevated temperatures, it can lead to problems such as the permanent

formation of conductive filaments or the breakdown of the dielectric layer, reducing the device's lifespan and endurance [Liu et al. \(2013\)](#).

Environmental factors such as temperature and humidity significantly influence the ionic dynamics and resistive switching behavior of memristors. For instance, increased temperature can enhance ionic mobility, thereby lowering the threshold voltage required for switching. However, it can also lead to increased leakage currents and reduced retention times due to accelerated diffusion and instability of the conductive filaments.

Humidity also plays a critical role, particularly in hygroscopic materials like PVP-coated nanowires. The absorption of moisture can rewire ionic pathways, facilitating or hindering filament formation. High humidity levels may lead to the hydrolysis of the electrolyte, degrading the device's performance over time.

The microscopic details of ionic migration are closely tied to the defect structures within the materials used in the device. In oxide-based memristors, for example, the concentration and distribution of oxygen vacancies heavily influence the switching behavior. Regions with a high concentration of defects can act as nucleation points for the formation of conductive filaments, which can lower the voltage required for switching [Ge and Chaker \(2017\)](#). Similarly, the way metal ions are distributed within the active layer can affect the uniformity and reliability of the switching process, which are critical for ensuring the performance of memory devices operating under stringent conditions.

3.2 Impact of Environmental Factors on Memristive Behavior

Memristors, short for memory resistors, are a type of two-terminal electrical component that stands out because of their ability to remember past electrical states. This unique characteristic has made them an essential part of neuromorphic computing and next-generation memory devices. [Chua \(1971\)](#) Memristive devices have attracted significant attention for their potential in a wide range of applications, including non-volatile memory, logic circuits, and even artificial synapses in neural networks (Fig. 3.3). However, one of the challenges with memristors is that their performance can be affected by environmental conditions. Understanding how factors like temperature, humidity, and atmospheric pressure influence their behaviour is crucial for improving their performance and ensuring their reliability in practical applications.

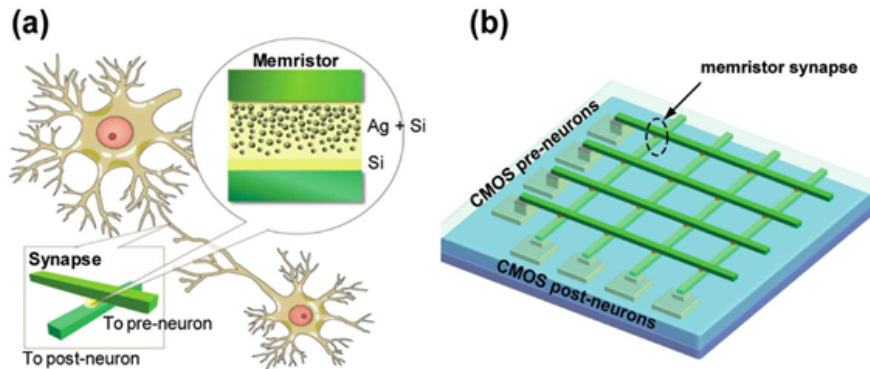


Figure 3.3: a) Structural similarity of memristor and neural connections b) crossbar array structure [Kuncic and Nakayama \(2021\)](#)

Temperature is a key environmental factor that significantly affects memristive properties, especially in devices that rely on ionic motion, filamentary switching, or phase changes. For instance, in metal-oxide memristors, temperature can influence the way conductive filaments form and dissolve, which directly impacts the switching between resistive states. Higher temperatures tend to speed up the movement of ions, which can alter the switching speed and the voltage thresholds needed for the memristor to switch states. However, prolonged exposure to high temperatures can cause material degradation, leading to unstable resistive states and a shorter device lifespan. Studies have shown that repeated exposure to heat, known as thermal cycling, can damage the oxide layers in memristive devices, potentially causing them to fail. [Xue et al. \(2019a\)](#); [Zhang et al. \(2012\)](#)

Humidity is another environmental factor that has a notable effect on memristive behaviour, especially in organic and polymer-based memristors. When moisture from the environment enters the device, it can be absorbed into the active layers, which disrupts the ionic pathways and changes how the device switches between states. In fact, high humidity has been shown to lower the voltages needed to switch states and increase the likelihood of leakage currents in organic memristive devices because water-associated ions become more mobile. Due to this sensitivity, it's important to use proper encapsulation methods to protect memristors from moisture, ensuring they perform consistently in different environments. [Zhang et al. \(2021\)](#); [Yang et al. \(2024\)](#)

Apart from temperature and humidity, atmospheric pressure can also influence the

behaviour of memristive devices. Pressure changes, especially in vacuum environments, can impact the movement of oxygen vacancies in metal-oxide memristors, which play a crucial role in the resistive switching process. Low pressure tends to enhance the retention of these oxygen vacancies, leading to more stable resistive states. On the other hand, higher pressure may introduce additional scattering centers that can degrade the device's performance over time. [Fernandes et al. \(2024\)](#)

Other environmental factors, such as exposure to electromagnetic radiation and mechanical stress, can also impact memristor performance. For instance, radiation can create defects in the materials that make up the memristor, which can either improve or impair its switching behaviour depending on the type and energy of the radiation. Additionally, mechanical stress, especially in flexible or stretchable memristive devices, can change the conductive pathways within the device, affecting its resistance states. This is particularly important to consider for memristors used in wearable electronics, where flexibility and durability are key factors. [Pattnaik et al. \(2023\)](#)

3.3 Predictive Modeling of Ion Dynamics in Memristive Devices with MCS

Monte Carlo simulations (MCS) represent a crucial computational approach for understanding and predicting the complex ion dynamics that underlie the operation of memristive devices. These simulations excel in capturing the stochastic processes involved in ion migration and filament formation, providing a detailed look at how these phenomena impact the performance and reliability of nanowire-based systems.

3.3.1 Understanding Monte Carlo Simulations in Ion Dynamics

Monte Carlo simulations are a versatile tool for modelling systems characterized by a high degree of randomness or complexity. From the perspective of memristive devices, these simulations are invaluable for exploring the dynamics of ion migration and filament formation—processes that are inherently probabilistic in nature. The primary strength of Monte Carlo methods lies in their ability to simulate the intricate movements of ions within a nanowire network, influenced by factors such as electric fields, temperature variations, and material imperfections. [Reinaudi et al. \(2020\)](#)

The basic methodology of Monte Carlo simulations involves several key steps:

1. **Initialization:** The process begins by setting up the initial state of the system, which includes defining the positions of ions within the nanowire network, establishing the initial distribution of the electric field, and setting the system temperature.
2. **Random Sampling:** The core of Monte Carlo simulations is the use of random sampling to determine possible ion movements. These movements are driven by probability distributions that reflect physical processes like diffusion, drift under an electric field, and scattering. The likelihood of various ion movements is influenced by local factors such as the electric field strength and thermal energy.
3. **Energy Calculation:** The energy associated with each possible state is calculated using the Boltzmann distribution:

$$P(E) = \frac{e^{-E/k_B T}}{F}$$

where E represents the energy of the state, k_B is the Boltzmann constant, T is the temperature, and F is the partition function, which accounts for all possible states. This formula ensures that states with lower energy are more probable, in line with thermodynamic principles.[Pathria and Beale \(2011\)](#)

4. **Iteration and Convergence:** The simulation iterates over many cycles, allowing the system to evolve and eventually reach equilibrium. The outcome is a statistically accurate representation of the ion distribution and the resulting filament formation within the memristor.[Wagner and Kliem \(2011\)](#)

3.3.2 Modeling Ionic Dynamics and Filament Formation in Memristors

In memristive devices, ionic dynamics play a pivotal role in enabling resistive switching, which is essential for the device's operation. Monte Carlo simulations are employed to model how ions migrate under an applied electric field and how these migrations lead to the formation of conductive filaments that bridge the electrodes.[Aldana et al. \(2020\)](#)

In metal-oxide memristors, oxygen vacancies serve as mobile charge carriers. Under the influence of an electric field, these vacancies migrate towards the anode, where they

accumulate and form a conductive filament. This filament, in turn, switches the device from a high-resistance state (HRS) to a low-resistance state (LRS). Shown in Figure 3.4 Monte Carlo simulations provide insights into the specific conditions—such as the critical voltage and temperature—that facilitate this filament formation. [Aldana et al. \(2018\)](#)

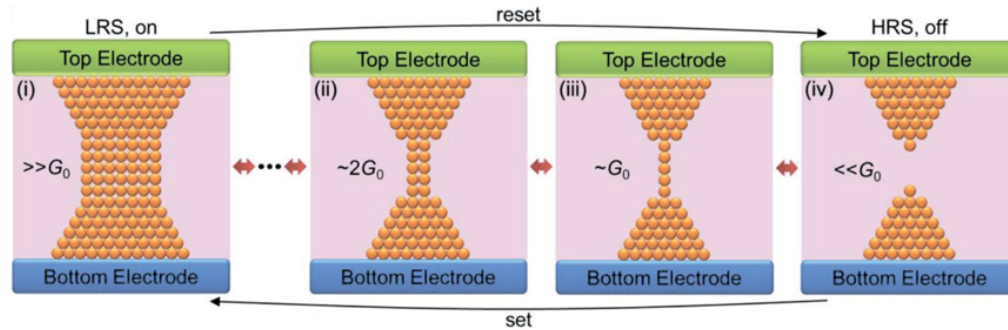


Figure 3.4: Development of quantum filament [Xue et al. \(2019a\)](#)

In stage (i), the filament is fully formed, providing a continuous conductive path between the top and bottom electrodes. This configuration corresponds to the low-resistance state (LRS) of the device, where the conductance is much greater than the quantum of conductance G_0 . The filament consists of a dense arrangement of atoms, ensuring efficient electron transport across the electrodes. [Xue et al. \(2019b\)](#)

As the reset process begins, the filament starts getting narrow, reducing the cross-sectional area available for electron transport. This state (ii) still allows conduction, but the conductance has decreased to approximately twice the quantum of conductance ($\sim 2G_0$). This stage represents a partial dissolution of the filament.

Further progression of the reset process leads to a significant narrowing of the filament, with conductance dropping to approximately the quantum of conductance (G_0). At this point (iii), the filament is almost dissolved, and only a thin connection remains between the electrodes. This state represents the transition from LRS to HRS, where the resistance is increasing, but a small conductive path still exists.

In the final stage (iv) the filament is fully dissolved, breaking the conductive path between the top and bottom electrodes. The device is now in the high-resistance state (HRS), where the conductance is much less than the quantum of conductance ($< G_0$). This state corresponds to the “off” state of the memristor, where the resistance is

maximized, and the device effectively blocks current flow.

When the polarity of the applied voltage is reversed, the conductive filament begins to dissolve, as the ions migrate back toward their initial positions. This dissolution returns the device to its high-resistance state. Monte Carlo simulations are crucial in modelling this process, as they help predict the reliability and stability of the device over multiple switching cycles. [Aldana et al. \(2020, 2018\)](#)

3.3.3 Applying Monte Carlo Simulations to Silver Nanowires

Ag NWs integration within memristors would lead Ag^+ ions within these nanowires to migrate in response to an electric field, forming and dissolving conductive filaments that enable the resistive switching behaviour essential for device operation. Monte Carlo simulations of Ag nanowires possibly can focus on modelling the migration of Ag^+ ions, predicting how these ions will aggregate under an electric field to form a filament, and how they will dissolve when the field is reversed. The simulations provide critical insights into the conditions required for reliable filament formation, including factors like threshold voltage, temperature, and the presence of impurities or structural defects within the nanowires [Reinaudi et al. \(2020\)](#).

Ag NWs integrated into the memristive devices coating of PVP will act as a stabilizing agent by introducing additional barriers to ion migration. Monte Carlo simulations can model the impact of these barriers, predicting how they influence the filament formation process. At lower temperatures, the simulations might show that these barriers slow down ion migration, resulting in more stable but slower switching behaviour. At higher temperatures, however, the simulations might predict faster ion migration, but with the potential risk of filament overgrowth, which could compromise the device's longevity.

The process of filament formation and dissolution in Ag nanowire-based memristors can be directly related to the quantum filament formation, as the simulation progresses, the stages of filament growth in Ag nanowires will reflect the quantum conductance changes. With possible research with application of Monte Carlo methods on Ag NWs may carry an important role in optimizing memristive devices for practical applications, ensuring their efficiency and reliability in next-generation memory and computing technologies.

3.4 ZnO nanowires characteristics under various impact of environment

Zinc oxide (ZnO) nanowires (NWs) have garnered significant attention due to their unique electrical, optical, and mechanical properties, making them promising candidates for a wide range of applications, including field-effect transistors, sensors, photovoltaics, and, notably, memristive devices. The behaviour of ZnO NWs, particularly in memristive applications, is highly sensitive to environmental factors, especially moisture. The research explores the influence of environmental conditions on ZnO NW characteristics, drawing on insights from two key studies that examine the impact of moisture on resistive switching behavior and the structural properties of ZnO in various forms. [Milano et al. \(2020b\)](#)

ZnO Nanowires in Memristive Devices

Memristive devices are a class of non-volatile memory that rely on resistive switching mechanisms, where the resistance of the device can be altered between high and low states by the application of an external voltage. ZnO NWs, owing to their high surface-to-volume ratio and crystalline structure, are particularly well-suited for such applications. In memristive devices based on the electrochemical metallization memory (ECM) effect, the switching mechanism involves the dissolution of metal atoms (such as silver) from an active electrode and their migration within the insulating ZnO matrix to form a conductive filament. This filament is responsible for the change in resistance. [Milano et al. \(2021\)](#)

Influence of Moisture on Resistive Switching

Moisture plays a dual role in influencing the resistive switching behaviour of ZnO NWs. On one hand, moisture adsorbed onto the surface of ZnO NWs can decrease electronic conductivity by creating a depleted region with upward band bending, which increases the overall resistance of the NWs. On the other hand, moisture can facilitate the migration of Ag⁺ ions by reducing the energy barriers for ion migration along the NW surface. This dual nature of moisture's influence was highlighted in a study where water molecules were found to reduce the electroforming voltage needed to establish a conductive path in ZnO NW-based memristive devices. [Milano et al. \(2021\)](#)

In ZnO NWs, the presence of moisture was observed to lower the forming and SET voltages, essential parameters in memristive devices. The lower voltages are attributed

to the water molecules adsorbed on the ZnO surface, which not only reduce the energy barrier for Ag⁺ ion migration but also increase the mobility of these ions. This increased mobility enhances the formation of a stable conductive filament, leading to more reliable switching behaviour. [Milano et al. \(2020b\)](#); [Patil et al. \(2023\)](#)

Structural Dependence and Comparison with ZnO Thin Films

The influence of moisture on ZnO NWs can be compared with its effects on ZnO thin films, which have also been widely studied for memristive applications. In ZnO thin films, particularly those created by sputtering and chemical vapor deposition (CVD), moisture impacts the resistive switching behavior in a manner similar to ZnO NWs. However, the extent of this impact is highly dependent on the structural properties of the ZnO film. Sputtered ZnO films, with their smaller grain sizes and larger number of grain boundaries, show a more pronounced response to moisture. This is because the increased number of grain boundaries in sputtered films provides more sites for moisture adsorption, thereby facilitating more pathways for ion migration. [Milano et al. \(2020b\)](#); [Panisilvam et al. \(2024\)](#)

In contrast, CVD-grown ZnO films, which have larger grain sizes and fewer grain boundaries, exhibit a less significant response to moisture. This structural dependence highlights the importance of grain size and boundary density in determining the sensitivity of ZnO-based memristive devices to environmental conditions. For ZnO NWs, which naturally have a high surface-to-volume ratio and few grain boundaries, the impact of moisture is primarily governed by surface adsorption effects rather than grain boundary interactions.

Mechanisms of Moisture Influence

The mechanisms by which moisture affects ZnO NWs and thin films are rooted in basic electrochemical principles. In a memristive device, moisture can participate in both anodic and cathodic reactions. For example, at the anode, moisture can facilitate the dissolution of silver into Ag⁺ ions, which then migrate through the ZnO matrix. At the cathode, moisture can participate in reduction reactions that maintain the overall charge balance within the device. This dual participation not only lowers the energy required for ion migration but also stabilizes the conductive filaments formed during the SET process. [Milano et al. \(2020b, 2021\)](#)

Moreover, moisture's ability to form a hydrogen-bond network along grain boundaries or on the surface of ZnO NWs further reduces the diffusion barriers for Ag⁺ ions.

This results in more efficient ion transport and a more pronounced resistive switching behaviour. The presence of moisture also influences the ON/OFF resistance ratio, with higher moisture levels typically leading to a higher ratio due to the enhanced mobility of Ag^+ ions and the more effective formation and rupture of conductive filaments.

3.5 Challenges in Nanowire Fabrication and Application

Despite their potential, several challenges must be addressed to scale nanowire networks for commercial use. These challenges, particularly related to environmental conditions, significantly affect both the fabrication and application of nanowire-based devices. This section explores the key challenges, emphasizing precision in fabrication, material selection, environmental stability, scalability, and mechanical integrity.

1. Precision and Control in Nanowire Fabrication

Achieving precise control over the size, shape, and orientation of nanowires is one of the foremost challenges in fabrication. Nanowires are typically on the order of tens of nanometers in diameter and extend several micrometres in length. Maintaining uniformity in these structural properties during fabrication is difficult, especially since variations in diameter, length, or crystallinity can lead to inconsistent device performance, particularly in applications where precise electrical or thermal properties are essential [Lee et al. \(2000\)](#). Different methods, such as chemical vapour deposition (CVD), solution-phase synthesis, and template-assisted growth, are used to produce nanowires, but each method has its own limitations. For instance, CVD can yield high-quality nanowires with good control over crystallinity, but it is challenging and expensive to scale. On the other hand, solution-phase synthesis can be scaled more easily but often produces nanowires with more defects, which can reduce device performance [Arjmand et al. \(2022\)](#). Furthermore, aligning nanowires precisely during fabrication is challenging but necessary, particularly in electronics. Techniques like nanoimprint lithography and dielectrophoresis have been developed to address alignment issues, but achieving consistent, cost-effective alignment at scale remains problematic. [Long et al. \(2012\)](#)

2. Material Selection and Compatibility

Choosing the right materials for nanowire networks presents another significant challenge. Different materials offer varying levels of conductivity, flexibility, and chemical stability. For example, silver (Ag) and copper (Cu) nanowires are highly conductive

and commonly used in transparent electrodes and flexible electronics. However, these metals are prone to oxidation, which degrades their electrical performance over time, especially in harsh environmental conditions such as high humidity or exposure to air. [Kou et al. \(2017\)](#) To address this, researchers have explored coating or alloying nanowires with protective materials, like gold (Au) or aluminium oxide “(Al₂O₃)”, to prevent oxidation. However, these protective measures can add complexity and cost to the fabrication process also they may alter memristive dynamics. Additionally, selecting materials compatible with flexible substrates that can maintain performance under mechanical stress is critical for applications like wearable electronics and flexible displays. [Xiang et al. \(2022\)](#)

3. Environmental Sensitivity and Stability

Environmental conditions such as temperature, humidity, and chemical exposure can significantly affect the performance and stability of nanowire networks. Due to their high surface-area-to-volume ratio, nanowires are highly susceptible to surface interactions with the environment. For instance, nanowires can undergo oxidation, corrosion, or surface contamination, all of which degrade their electrical properties and limit their long-term reliability. [Erol et al. \(2011\)](#) Humidity is a key environmental factor affecting nanowire networks. The adsorption of water molecules onto nanowire surfaces can alter electrical conductivity, particularly in materials like zinc oxide (ZnO) and silver, where humidity enhances ionic conduction or causes oxidation, leading to increased resistance and device failure. [Ma et al. \(2024\)](#) Ensuring the environmental stability of nanowire networks requires the development of effective encapsulation or passivation strategies to protect against moisture and contaminants. Temperature fluctuations also pose challenges, especially in applications where nanowire networks are exposed to varying thermal conditions. The small size of nanowires can lead to significant thermal expansion or contraction, which may cause mechanical failure, such as cracking or delamination in devices. [Salhi \(2020\)](#) Developing materials and device architectures that can accommodate thermal expansion or exhibit thermal stability across a wide range of temperatures is essential for the reliability of nanowire-based devices. These effects’ impact on NWNs is not fully clear yet, so further measurements by application of the cycles can be designed to find the answer. This thesis’s aim is also to find a correlation if any with a designed experiment that is explained in the next Chapter.

4. Scalability and Manufacturing

Scaling up nanowire network fabrication for commercial applications remains one of the most critical challenges. Although promising nanowire-based prototypes have been demonstrated in the lab, transitioning to mass production is far more complex. Achieving uniform nanowire production, ensuring consistent material properties, and developing cost-effective large-scale fabrication methods are hurdles that must be overcome [Sheng-Yun et al. \(2020\)](#). One major issue with scalability is producing large-area nanowire networks with uniform coverage and consistent performance. Coating techniques developed for depositing nanowires over large areas often may lead to random orientation and uneven distribution of nanowires, resulting in non-uniform electrical properties and suboptimal device performance, particularly in transparent conductive films and large-area sensors, especially in not well-controlled environments. [Kumar et al. \(2022\)](#) Moreover, integrating nanowire networks into existing manufacturing processes for electronics, optoelectronics, and sensors is challenging. Ensuring compatibility with standard lithography, integrating with flexible substrates, and establishing robust electrical contacts between nanowires and other components are critical considerations for developing commercial nanowire-based devices.

5. Mechanical Integrity and Reliability

The mechanical integrity and reliability of nanowire networks are crucial, particularly for applications in flexible electronics, wearable devices, and stretchable sensors. Nanowire networks need to maintain their electrical and mechanical properties under repeated bending, stretching, or compressing. However, nanowires are vulnerable to mechanical failure under strain. They may fracture, detach from the substrate, or lose contact with adjacent nanowires, leading to degraded performance over time. [Grazioli et al. \(2024\)](#) Researchers are exploring various strategies to improve mechanical reliability. These include embedding nanowires in flexible polymers, enhancing the mechanical properties of the nanowire materials, and developing stretchable architectures that can withstand mechanical deformation without breaking. [Prameswati et al. \(2022\)](#) These approaches aim to ensure that nanowire networks can endure the mechanical demands of flexible and wearable devices while maintaining their functionality.

3.6 Future Directions in Neuromorphic Computing

The field of neuromorphic computing has seen significant advancements, particularly with the development of memristor-based systems, phase-change materials and nanowire networks. Memristors, in particular, have shown great promise due to their ability to mimic synaptic behaviour by adjusting their resistance in response to electrical currents. This capability allows them to “remember” previous inputs, making them ideal for tasks such as learning and memory retention [Roy et al. \(2019\)](#).

Phase-change memory (PCM) devices, which utilize reversible phase transitions in chalcogenide materials, offer another avenue for neuromorphic computing. These devices can simulate the analog behaviour of synaptic weights, making them suitable for spiking neural networks (SNNs) that process information using time-dependent spikes, much like biological neurons [Raoux et al. \(2008\)](#). Spintronic devices, which exploit the spin of electrons in addition to their charge, provide yet another approach to neuromorphic computing. These devices are non-volatile, offering energy-efficient computation with persistent memory, making them ideal for real-time processing and adaptable neuromorphic circuits [Wolf et al. \(2001\)](#).

Ag NWNs are gaining attention for being scalable and suitable for large-scale neuromorphic systems that require high-density synaptic connections, making them particularly well-suited for RNNs that mimic biological neural activity [Diaz Alvarez et al. \(2019a\)](#).

Neuromorphic computing represents a significant leap forward in how computational systems are designed, inspired by the architecture and functions of the human brain. Traditional computing systems, based on the von Neumann architecture, separate memory and processing units, resulting in data transfer bottlenecks and higher energy consumption. In contrast, neuromorphic systems integrate memory and processing more closely, much like how biological neural networks function. This integration allows for more efficient and adaptive processing, essential for tasks such as pattern recognition, learning, and decision-making, which are critical in AI applications.

The concept of neuromorphic systems isn’t entirely new. It was first introduced by Carver Mead in the 1980s, who envisioned circuits that could emulate biological information processing using analog components rather than digital logic gates [Mead \(1990\)](#). This marked the beginning of a new paradigm in computing hardware, where the fo-

cus shifted towards mimicking the brain’s synaptic plasticity and parallel processing capabilities. The development of Metal Oxide Semiconductor Field Effect Transistors (MOSFETs) further advanced this field by enabling the creation of more sophisticated neuromorphic circuits.

Today, neuromorphic computing encompasses various novel nanotechnologies, including non-volatile memory devices and memristors, which can mimic synaptic behaviour [Waser et al. \(2019\)](#). These devices operate based on resistive switching mechanisms, where the resistance of the device changes in response to an applied voltage, much like how synapses adjust their strength based on neural activity. The unconventional “beyond von Neumann” architecture of these devices significantly reduces power requirements, making them ideal for implementing Artificial Neural Network (ANN) algorithms that replicate neuronal and synaptic connections in software [Hu and Li \(2022\)](#).

Current neuromorphic systems, such as IBM’s TrueNorth and Intel’s Loihi chips, are limited in their ability to fully replicate the complexity of biological neural networks. These systems primarily focus on integrating processing and memory to reduce power consumption but do not fully capture the emergent properties of neural networks, such as learning and memory, which arise from the network’s complex structure [Akopyan et al. \(2015\)](#). This limitation stems from the grid-like array structure of these systems, which emphasizes individual synapse-like elements rather than the overall network architecture. As a result, these systems lack the emergent dynamical properties that are characteristic of biological neural networks, such as small-world architecture and complex topologies [Chialvo \(2010\)](#).

To find the solution to these limitations, researchers have developed advanced neuromorphic systems composed of self-assembled nanowires that mimic the structure and function of biological neural networks. These Atomic Switch-like Networks (ASNs) utilize non-linear synaptic functions at the junctions between nanowires, similar to atomic switches [Terabe et al. \(2005\)](#). Unlike conventional neuromorphic systems, ASNs emphasize the emergent dynamical properties arising from their complex network topology, enabling them to mimic the brain’s adaptability and learning capabilities.

Chapter 4

Experiment design

4.1 Ag-PVP Nanowire Networks synthesis and main characteristics

4.1.1 Self organizing structure of Ag-PVP NWNs

Figure 4.1 provides a detailed look into how NW networks adapt and change through two key processes known as “reweighting” and “rewiring.” These processes are fundamental to the structural plasticity of the network, which is the ability of the network to change and adapt its structure in response to external electrical stimuli, much like how a brain might adjust its connections between neurons based on experiences [Milano et al. \(2022\)](#).

Figure 4.1a introduces the concept of “reweighting.” Consider two nanowires crossing each other, with a thin layer of insulating material between them. When a voltage is applied across these wires: silver ions start moving through this insulating layer, forming a tiny bridge that connects the two wires. This connection alters the resistance of the junction. This change in resistance is what we refer to as “reweighting,” and it’s crucial because it allows the network to adjust its electrical properties based on the signals it receives.

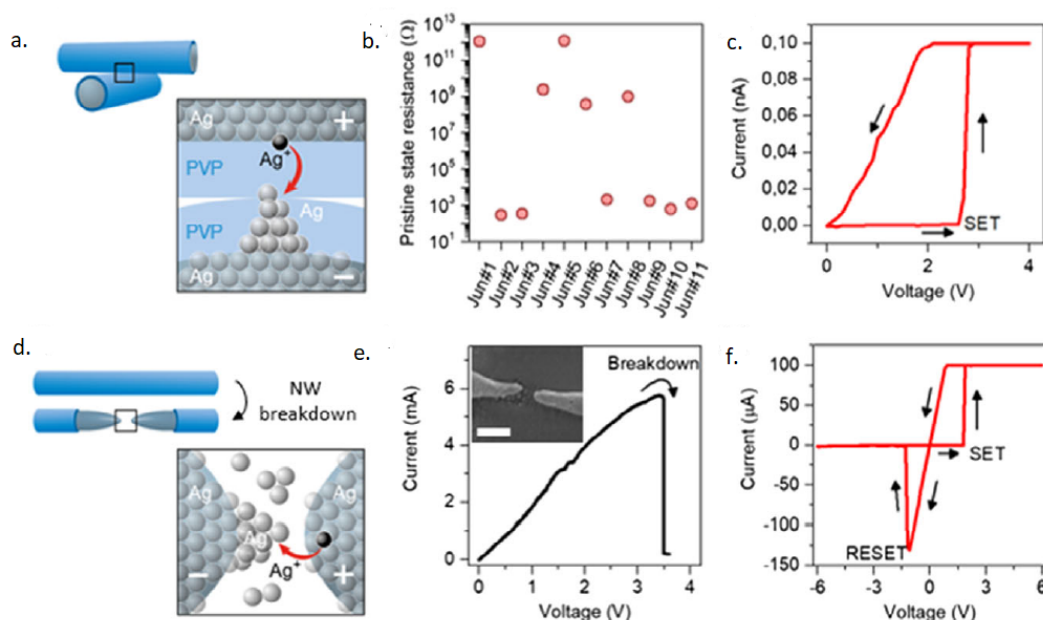


Figure 4.1: Explanation of “reweighting” and “rewiring” of single Ag NW [Milano et al. \(2022\)](#)

Figure 4.1b shows us that different NW junctions don’t all start from the same point. The initial resistance can vary widely from one junction to another. This variability is due to the way the wires touch each other sometimes where strong or weaker contacts may occur depending on the randomness of how the wires are positioned and the presence of a thin coating around them. This randomness is similar to how not all connections in the brain are equally strong, which adds to the complexity and adaptability of the system.

Further in Figure 4.1c, we gain a deeper understanding by observing what happens when a specific voltage is applied to a single NW junction. The resistance suddenly drops, which means that a conductive path has formed between the wires. This behaviour is a clear example of “reweighting” in action, where the network’s response to electrical input is fine-tuned.

Figure 4.1d shifts focus to the different concept that happens when a nanowire experiences a high electrical current. This current can cause the wire to break, creating a tiny gap known as a nanogap. They are not permanent damage since under the right conditions, the network can “heal” itself by forming a new conductive path across the gap. This ability to re-establish connections is what we refer to as “rewiring” [Manning et al. \(2018\)](#).

To confirm this process visually, Figure 4.1e includes an image obtained through a scanning electron microscope (SEM), showing the actual nanogap that forms after a breakdown event. In the last part, the Figure 4.1f presents how this nanogap behaves electrically. The current-voltage (I-V) graph displays a hysteresis loop, a signature of memristive behaviour, meaning that the network remembers the electrical history of the nanogap and can adjust its behaviour accordingly [Milano et al. \(2022\)](#).

All parts together give a brief explanation of how the NW network is dynamic and capable of adapting to different conditions. The processes of reweighting and rewiring enable the network to mimic the flexibility and learning capabilities of the brain, making it a promising technology for creating advanced, brain-like computing systems. Understanding these processes is essential because they highlight how the physical structure of a network can directly influence its ability to process and store information for neuromorphic computing.

4.1.2 Production of the Ag-PVP nanowires

For experiment, the memristive device made of silver nanowires (Ag NWs) thinly covered in an insulating polymer called polyvinylpyrrolidone (PVP) is used. This layer of polymer is very thin, usually measuring just one or two nanometers. PVP is essentially a leftover byproduct of the nanowire synthesis process. The insulating polymer layer, although a residue, is essential to the device's ability to display resistive switching behaviour. The most important aspect of the apparatus is the creation of a metal-insulator-metal (MIM) at the crossing points of the structure, which becomes achievable only by this behaviour.

The development technique for these Silver-PVP nanowire networks (Ag-PVP NWNs), as detailed in the group's works, is dropping Silver nanowires suspended in an alcohol solution, namely isopropyl alcohol (IPA), over a silicon dioxide SiO_2 substrate material. Areal mass density (AMD) of the coated nanowires that grow may be precisely monitored by varying the mass ratio of the nanowires to the IPA in the suspension [Milano et al. \(2020a\)](#). In simple terms, increasing the quantity of IPA correlates with a lowered AMD, as seen in Figure 4.2.

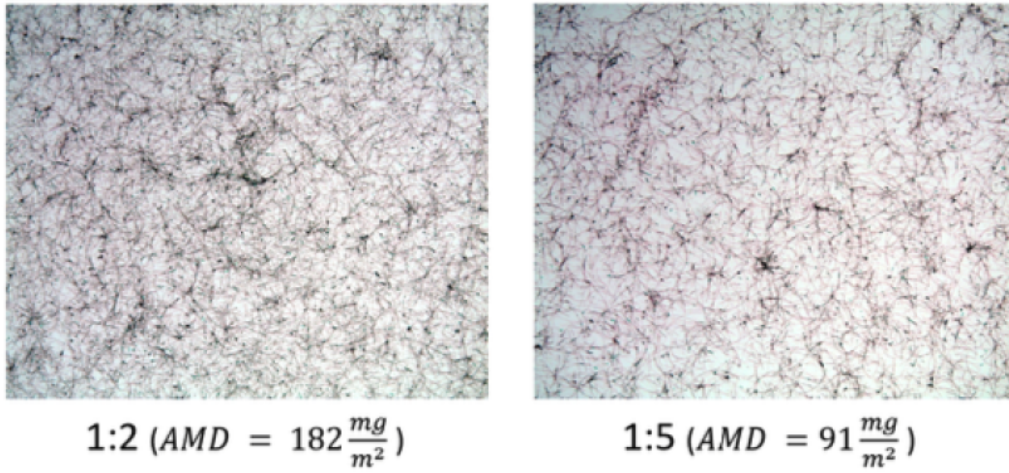


Figure 4.2: Samples with different nanowire densities [Milano et al. \(2020a\)](#)

To get a lower AMD, the nanowires are originally bought in an alcohol solution, which is then diluted with IPA. In this work’s case Ag NWs’ areal density is shown table below:

Sample	AMD ($\frac{\text{mg}}{\text{m}^2}$)
N171	182.73
N172	136.62

Table 4.1: Areal mass density of used samples in this work

After the nanowires have been formed, gold pads are sputter-deposited around the borders of the nanowire network to act as electrodes for network access. The pad regions are properly defined using a shadow mask. These pad positions are not exactly represented in the same way as the samples we used Figure 4.3 provides a thorough representation of them. Notably, the entire fabrication process is simple and inexpensive, as it does not demand cleanroom facilities or advanced lithographic processes.

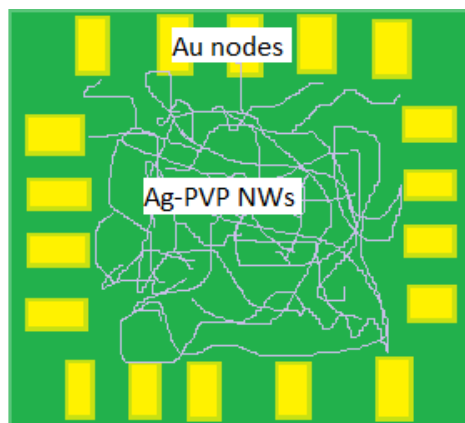


Figure 4.3: Diagram of gold deposition on corners

Below in Figure 4.4 a real image of the experiment's device is shown. The probes connected to the 3rd node from left and right, North and South accordingly. It is also obvious that during our experiment water droplets were formed due to the condensation on the surface of our measured device specifically during relative humidity cycles.

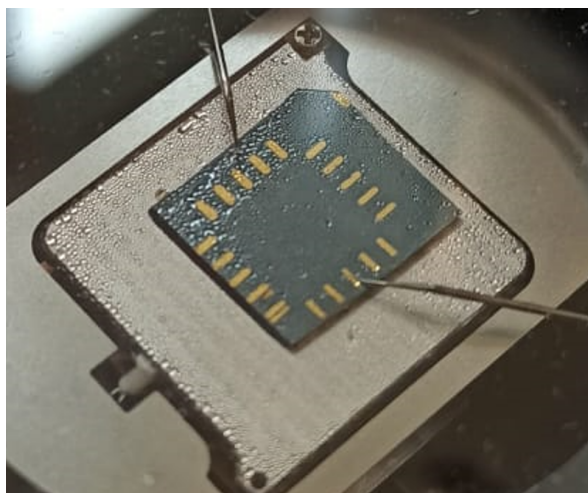


Figure 4.4: Reformed water droplets on nanowires due to condensation

4.2 Experimental Setup

In this experiment, the conductance of silver nanowire networks (AgNWs) is studied under controlled humidity and temperature conditions using a designed setup. The Precision Humidity Control System (HCS-2M) ensures precise humidity regulation, maintaining a range between 4-95% RH. This will create a controlled environment for observing how environmental humidity influences the electrical properties of nanowires. The chamber's temperature is regulated using Peltier technology, which offers both heating and cooling capabilities, covering a range from -40°C to 200°C .

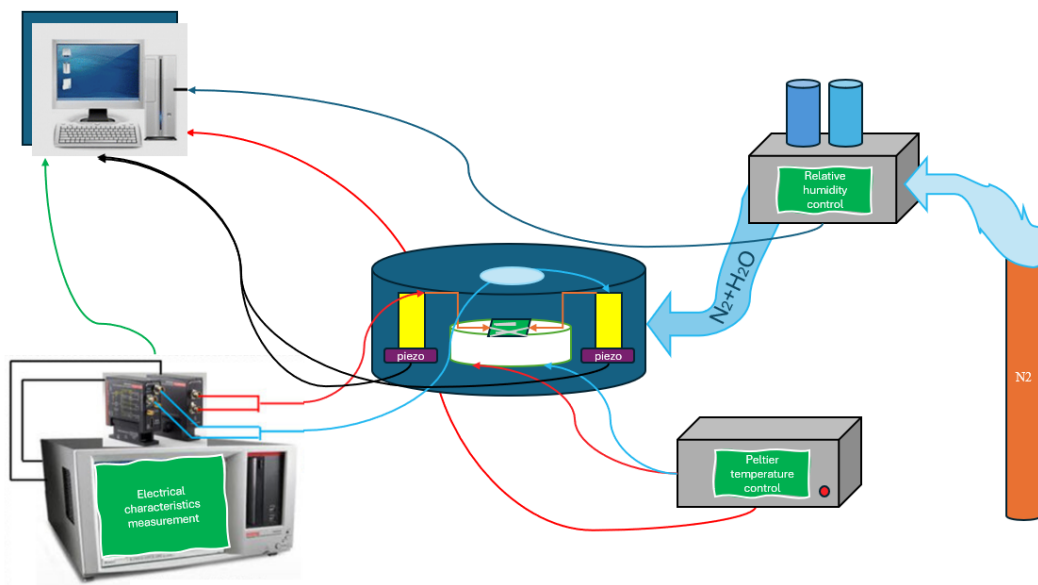


Figure 4.5: Experimental Setup

For the electrical characterization, a Keithley 4200-SCS Semiconductor Characterization System has been used which allows application of voltage pulses and real-time measurement of the nanowires' electrical response. The continuous measurement data capturing ability makes the system ideal for studying how the nanowires behave under different humidity levels and temperature cycles.

4.2.1 Controlling Relative Humidity

The Precision Humidity Control System (HCS-2M) offers precise PID (Proportional Integral Derivative) control and integrates a humidity sensor directly inside the mi-

croprobe stations (MPS) chambers. It maintains a normal ramp speed of 10% RH per minute and operates within a standard range of 4-95% RH, though this may vary depending on the specific experimental and lab conditions [MicroprobeSystems \(2024b\)](#).

The Temperature controller provides accurate control, with Peltier models allowing active cooling and special temperature profiles, while LN (Liquid Nitrogen) models include an LN circulation pump for low-temperature cooling.

4.2.2 Piezo-driven probe chamber for various heat applications and humid environments

This compact piezo-driven probe module offers high precision and control, suitable for delicate manipulations and measurements, with a high holding force and fine resolution, making it ideal for nanotechnology applications. The device also supports a wide range of operating temperatures, accommodating various experimental conditions

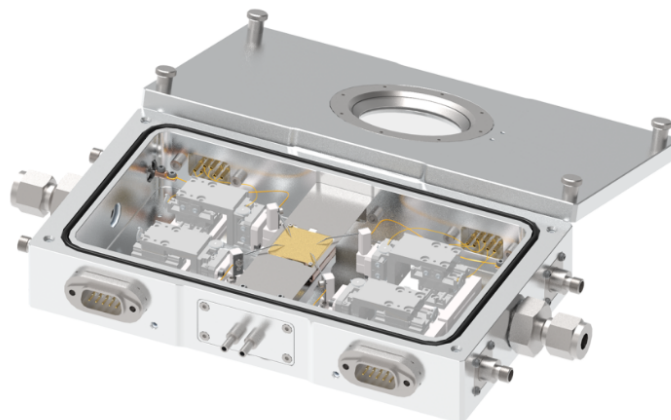


Figure 4.6: Piezo-driven chamber for many applications [MicroprobeSystems \(2024a\)](#).

The device features a module speed of 5 mm/s, with a stroke range of 8 mm on the X and Y axes and 3 mm on the Z-axis. The probe can exert a holding force of 250 to 300 gf, making it suitable for careful tasks. It operates with high precision, offering a resolution of less than 1 μm . The system is capable of functioning across a wide temperature range, including cryogenic and high-temperature conditions. For example, the range of temperature application with the help of Peltier effect is -40 up to the 200 C. [MicroprobeSystems \(2024a\)](#)

4.2.3 Electrical characterization measurements of the nanowires

Keithley 4200-SCS Semiconductor Characterization System integrated with the 4225-RPM offered comprehensive data acquisition and analysis tools. It enabled us to record the conductance of the nanowires with high precision and to analyze the data in real time. The system's range of measurement allowed us to perform a wide range of tests, from basic maximum conductance and time measurements to more complex pulse-based characterizations. [Instruments \(2018\)](#)

4.2.4 Experimental steps

1. Sample Preparation:

Ag-PVP NW networks are fabricated and then the ready device is carefully placed inside the chamber.

2. Microprobe Contact:

Using the piezo motor-driven microprobe system, precise contacts are made with the sputtered electrodes that contact random NWs. As shown previously in Figure 4.4 central (3rd) electrodes facing each other connected to probes. The position and pressure of the probes are adjusted to ensure a stable and consistent electrical connection.

3. Electrical Measurement:

The Keithley 4200-SCS is configured for I-V measurements. The Keithley 4225-RPM unit applies electrical pulses and measures the resulting current through the NW networks. Measurements are taken at different humidity levels and different cycles of the temperature sweeps to observe what are their effect on the non-linearity of the nanowires we produced.

4. Humidity and Temperature control:

Humidity is set using the Nextron HCS-2M system being connected to the chamber. Temperature is controlled by Peltier connected to the surface under the nanowire network chip. All these cycles automated by software provided Noxtron with predefined steps of their humidity and temperature controllers which are mentioned above.

5. Data Collection and Analysis:

The collected data is analyzed through a computer in Python programming language to determine the relationship between humidity/temperature and the electrical conductance of the Ag-PVP NWN by plotting them at parallel time. So in case of any event where we can't see the potentiation or relaxation, tuning of the pulse voltage can be redone and we can convert our measurements only when correlated with nanowire dynamic behaviour.

6. Safety and Precautions:

Handling the microprobes with extreme care to avoid damaging the nanowires. Using a shield to block light and matter interactions on the surface of the nanowires, to expand their lifetime of performance.

Chapter 5

Results

5.1 Measurements with continuous V applied

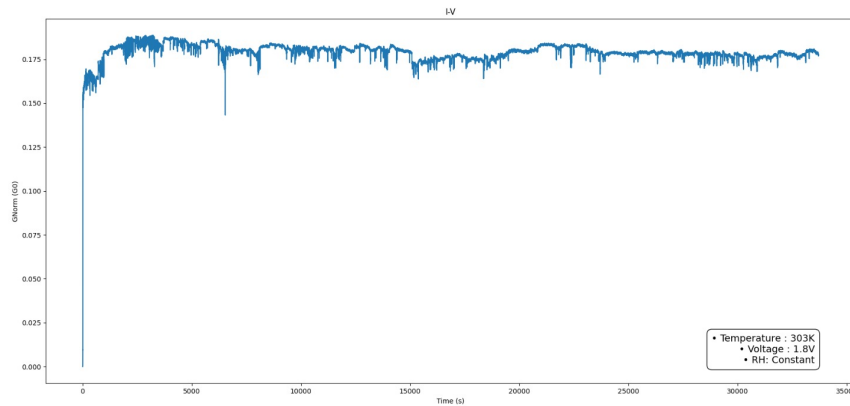


Figure 5.1: Change of G_0 during T,RH,V const

Figure 5.1 demonstrates G_0 , conductance change during time. In this measurement, constant voltage $V=1.8V$ was applied to nanowire networks to nodes as shown in Figure 4.4. As we can see first point of the time presents a pike in conductance due to the application of voltage. The temperature was fixed at 30C, also relative humidity was constant since the measurement was held on an isolated cryostat, there was no significant change in the behaviour of conductance.

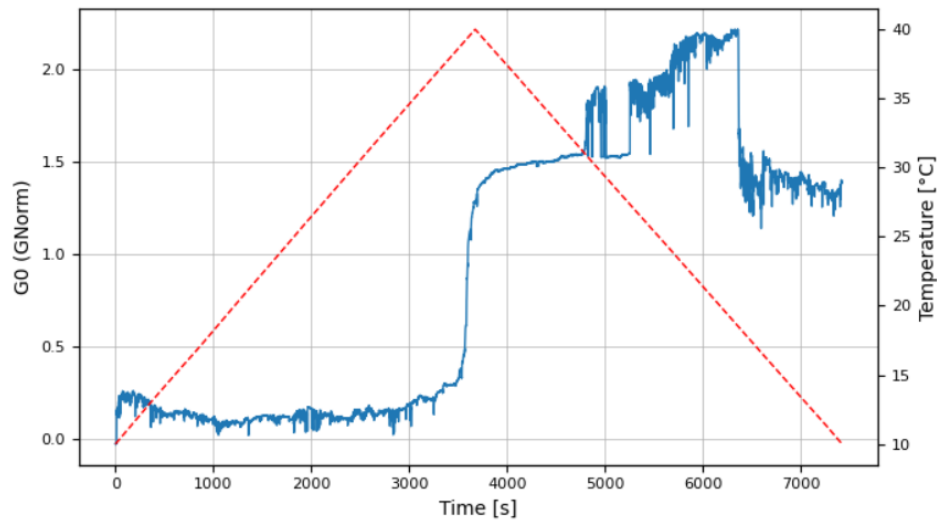


Figure 5.2: Change of G_0 during T cycle (10-40-10C)

Similar to the previous one, Figure 5.2 represents G_0 conductance on the y-axis and time on the x-axis, applied voltage was continuous as before but 0.5V. During measurements of sample N171 relative humidity was kept constant at 60%. Temperature continuously cycled from 10 to 40 C and back to 10 C. As we can deduct from the graph when the temperature reaches the highest value (40 C) high temperature favours a step in conductance.

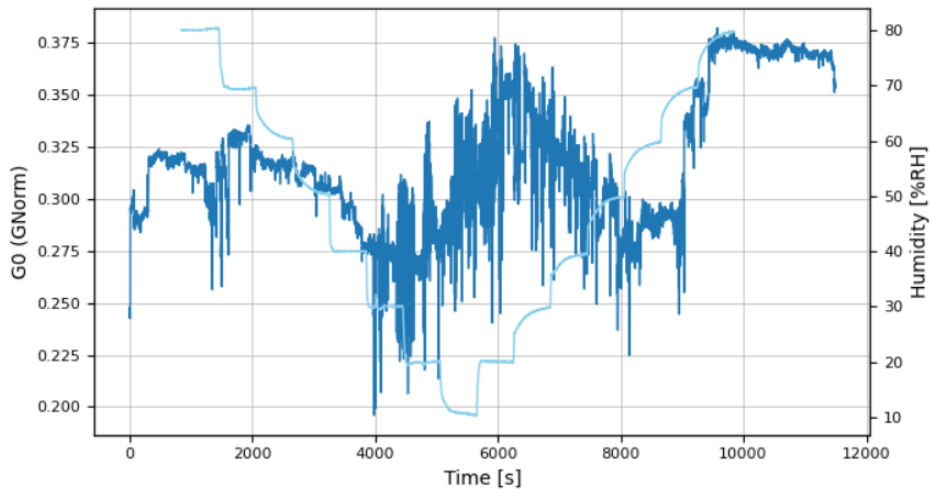


Figure 5.3: Change of G_{norm} during RH cycle (80-10-80%)

In Figure 5.3 conductance values are plotted with the application of constant Voltage

(0.5V). This time temperature is fixed at 300K. Relative Humidity cycled from 80% to 10% and back to 80%. It is present in the graph how low humidity produces more spiky dynamics but it is reversible going up high relative humidity (80%).

5.2 Relative humidity effects on Ag-PVP potentiation

At the next step of the experiment sample N172T was used, for each point of the temperature cycle, 7 V of voltage pulse for 10 seconds was applied, and each measurement for each relative humidity level roughly took 10 minutes. The goal was to observe how the maximum conductance (G_{\max}) of the sample evolved during the humidity cycle, with humidity ranging from 80% to 30% and then back to 80%, while keeping the temperature constant at 27°C.

5.2.1 G_{\max} vs Time

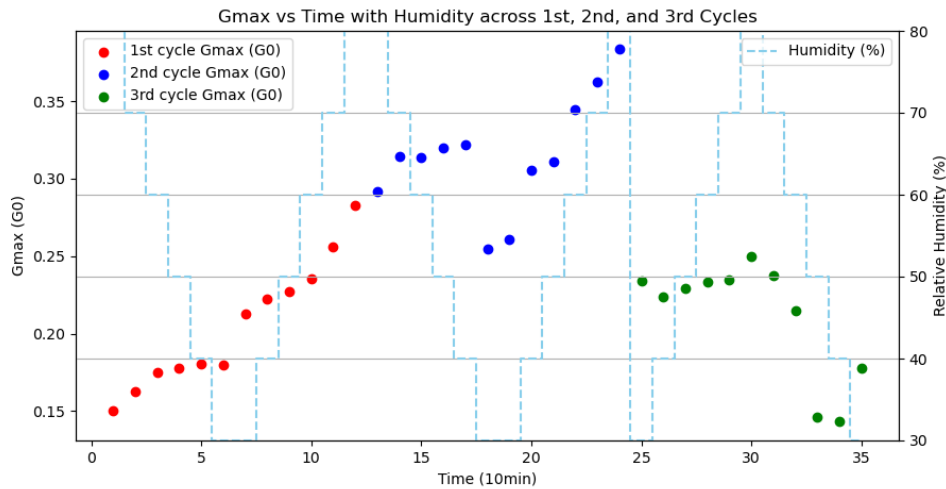


Figure 5.4: G_{\max} vs Time

From the graph Fig. 5.4, it's evident that G_{\max} increased consistently over time, there is a continuous long-term modification that is independent of the humidity given by repeated voltage application. Each colour represents one cycle of RH (80-30-80%), and it should be also kept in mind the last cycle of this measurement is done in the

reverse cycle. But in the case of all three cycles, it's not determined how humidity directly affected the behaviour of Ag NWNs.

5.2.2 ΔG_0 vs Time

Results reported in Fig. 5.5, the change in conductance ΔG_0 over time was measured under the same conditions of varying humidity, sample N172T displayed a gradual increase in ΔG_0 over time, specifically when it reached 3rd cycle of humidity, presenting chaotic data. 1st cycle shows a sudden peak during 2nd half of the cycle while the transition from 30 to 40% RH, 2nd cycle (blue) generally supports decreasing humidity causing a decline in ΔG_0 value.

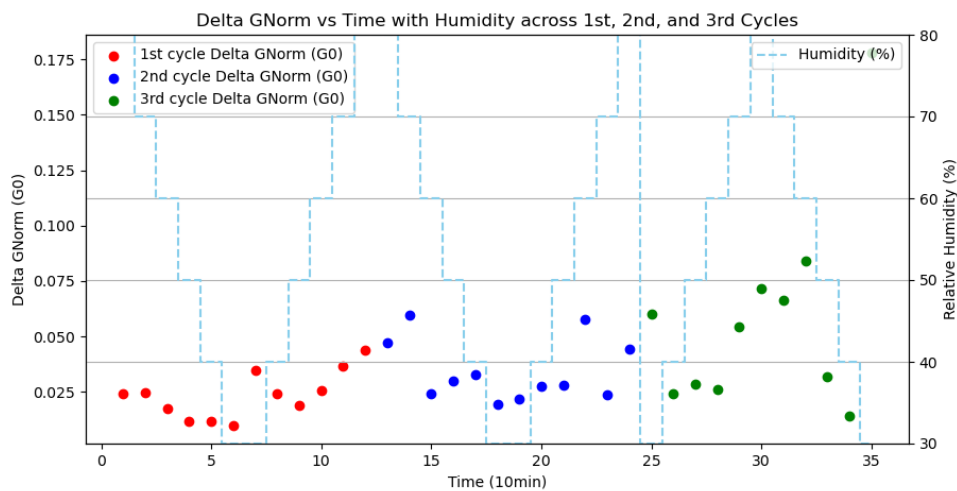


Figure 5.5: ΔG_0 vs Time

5.2.3 G_{\max} vs Relative Humidity

Figure 5.6 shows as the humidity was cycled the conductance values were recorded at various points. The G_{\max} decreased with decreasing humidity and showed the lowest values at lower humidity levels. But while cycling back to high humidity at some cycles it shows less value, which can be related to reforming new paths through nanowire networks with increasing humidity. The behaviour of sample N172T unfortunately didn't allow for clear observations of how humidity impacts the conductive properties of the nanowires.

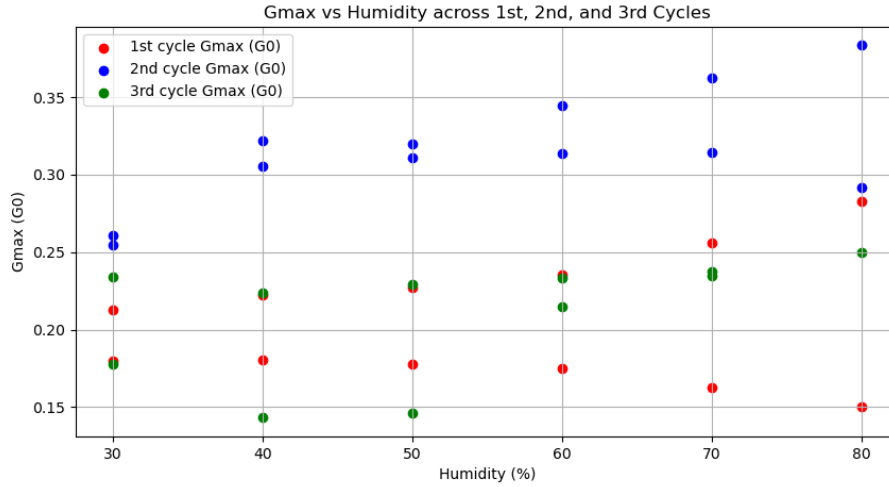


Figure 5.6: G_{\max} vs Relative Humidity

5.2.4 ΔG_0 vs Relative Humidity

Figure 5.7 illustrates the relationship between the humidity decrease, and the change in conductance since mentioned in the previous Fig. 5.6 explanation sample N172T shows fluctuations at different humidity levels which creates difficulty in building correlation.

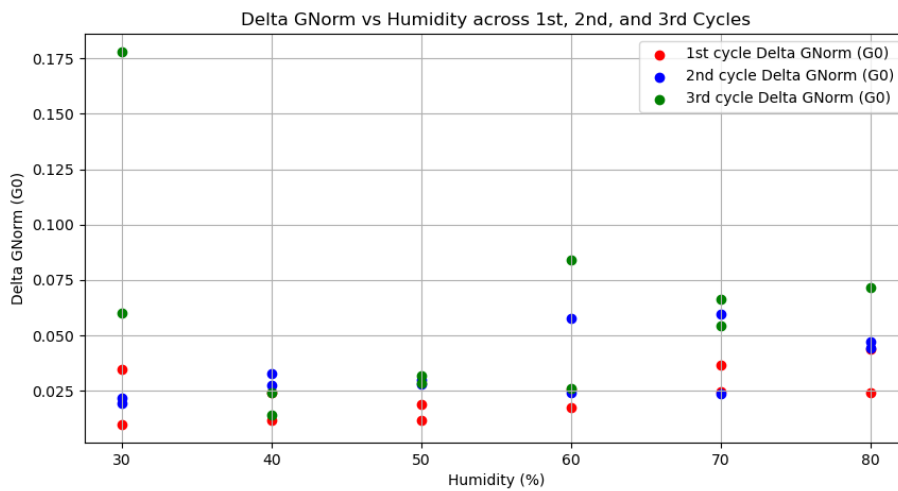


Figure 5.7: ΔG_0 vs Relative Humidity

5.2.5 Average ΔG_0 vs Relative Humidity

Fig. 5.8 presents the average ΔG_0 against relative humidity while providing a broader view of how relative humidity influences the conductance across different conditions. The observed trend shows a consistent increase in average conductance as humidity increases, despite all measurement results being compatible. But as can be seen dynamics of the sample N172T show various fluctuations.

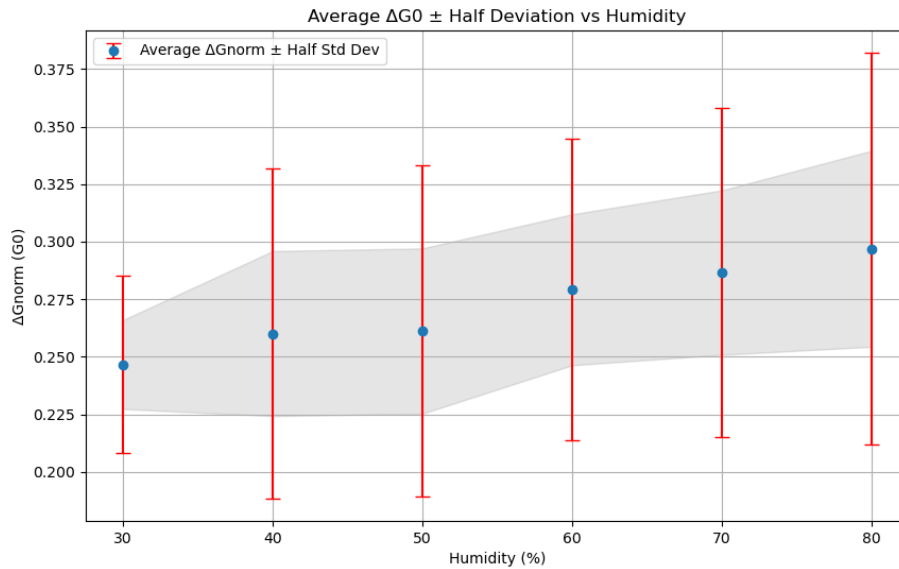


Figure 5.8: Average G_0 vs Relative Humidity

The increase in conductance with higher humidity could have possible causes that are mentioned in previous chapters in this work. Water molecules that are adsorbed by the surface can create hydroxide ions (OH^-). Ions initiate redox reactions on the surface of the silver nanowires and the oxidation of silver (Ag) to silver ions (Ag^+). This dynamic redox activity enhances conductance by increasing the number of charge carriers within the network. Another reason is an increase in ionic mobility because water molecules lower the energy barrier for migration which correlates to higher conductance. Humidity can alter the surface charge distribution and modify the local electric field around the nanowires. This change can enhance the overall connectivity of the network or assist in the formation of conductive filaments between nanowires.

5.3 Temperature effects on Ag-PVP potentiation

In this part of the experiments, since we measure temperature effects, RH is fixed at 60% and with the help of the Nextron temperature controller, values are assigned to temperature with 5C steps. The temperature started from 10 C and reached 40 C max for this experiment and cooled back to 10 C. Throughout the process, the humidity was kept constant at 60%. It's worth mentioning that I initially started with sample 172N but had to switch to sample 171N because it exhibited better consistency and stability of data. For each point of the temperature cycle, 0.5 V of voltage pulse for 10 seconds was applied, and each measurement for each temperature roughly took 10 minutes.

5.3.1 G_{\max} vs Time across Cycles

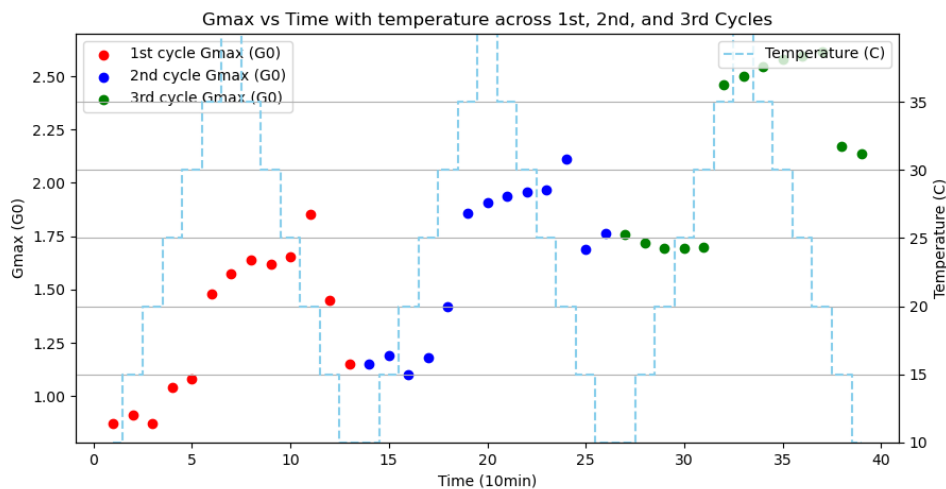


Figure 5.9: G_{\max} vs Time

Figure 5.9 demonstrates how the temperature cycle was repeated 3 times. During each cycle (G_{\max} increases noticeably during heating from 10C to 40C. However, during the reverse cycle (cooling down) maximum conductance for several steps keeps increasing reaches its maximum value and decreases while temperature decreases. This behaviour indicates the possibility that the nanowire network was experiencing an initial surge in conductance before possibly stabilizing or even degrading a bit over time. This should be kept in mind that the network keeps potentiating in general, it is only the

potentiation effect of each pulse that remains the same, which is the outcome of the cycle transition in the given graph.

5.3.2 ΔG_0 vs Time across Cycles

When looking at Figure 5.10, it is clear that ΔG_0 increased initially in each cycle. But as time went on while the temperature increased, it either stabilized or began to decline. The first cycle (red) is the opposite in the case of G_{\max} relationship against time. ΔG_0 decreases while increasing temperature and returns to similar initial values when temperature decreases. 2nd cycle tries to implement the same behaviour but ends unsuccessfully since does not reach close to the initial values. During 3rd cycle (green) difference in conductance maximum and minimum values is not affected between the change of the initial and last steps of the cycle, but at the highest value of the temperature is different than the first 2 cycles it represents its highest value instead of the lowest.

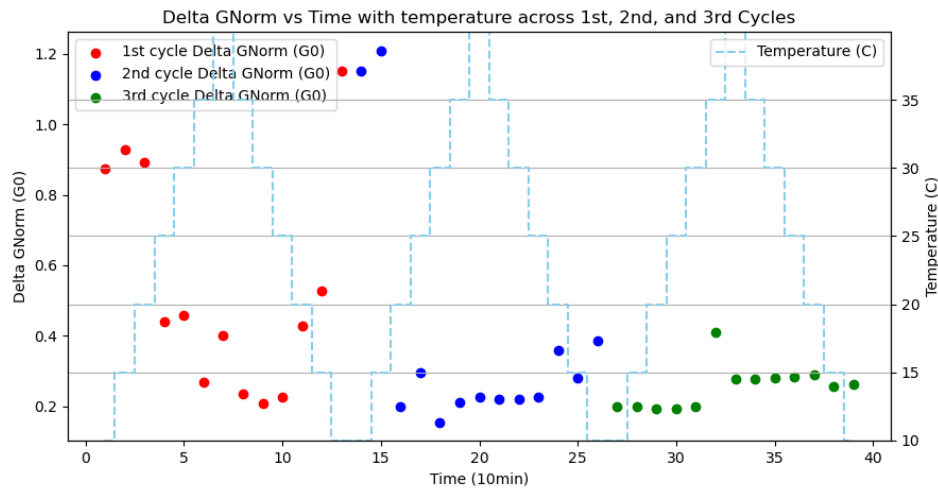
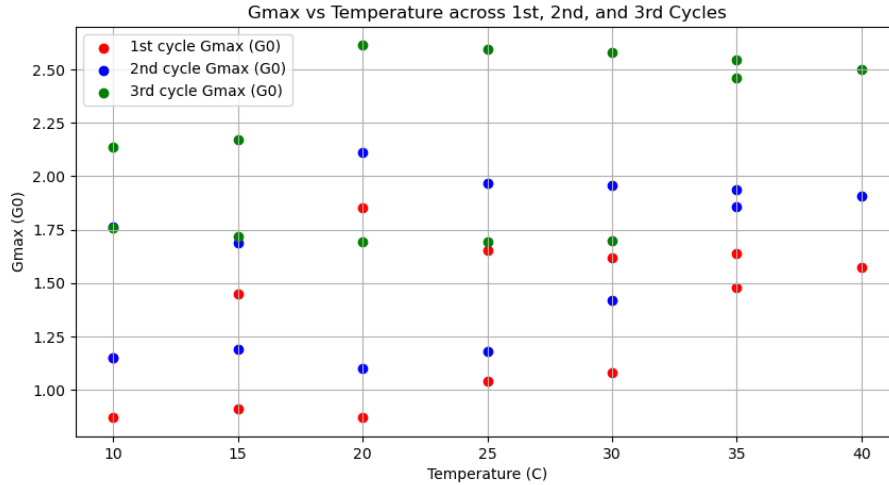


Figure 5.10: ΔG_0 vs Time

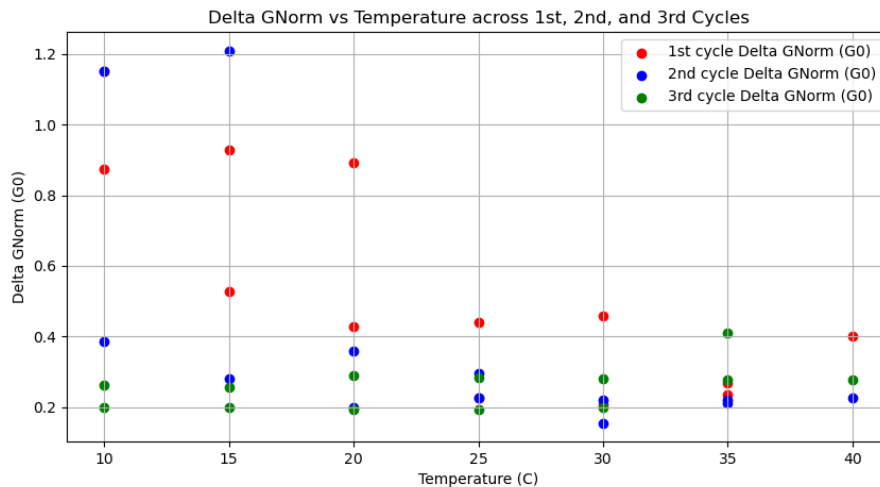
5.3.3 G_{\max} vs Temperature across Cycles

The 5.11 graph presented a variety of trends in G_{\max} across different temperatures and cycles. Contrary to what one might expect, there wasn't a clear trend of maximum conductance increasing with temperature. Instead, G_{\max} seemed to either stabilize or

Figure 5.11: G_{\max} vs Temperature

even decrease at certain points, particularly after repeated cycling. But together with Figure 5.9, it can be explained that the network is generally potentiating without any kind of saturation.

5.3.4 ΔG_0 vs Temperature across Cycles

Figure 5.12: ΔG_0 vs Temperature

In Figure 5.12, ΔG_0 decreased with each successive cycle, particularly at the lower

temperatures. This pattern suggests that, with repeated exposure to these temperature cycles, the nanowire network might be adapting in a way that leads to smaller changes in conductance. It seemed like the network was becoming more stable, with established conductive pathways, which reduced the impact of further temperature cycling.

5.3.5 Average ΔG_0 vs Temperature

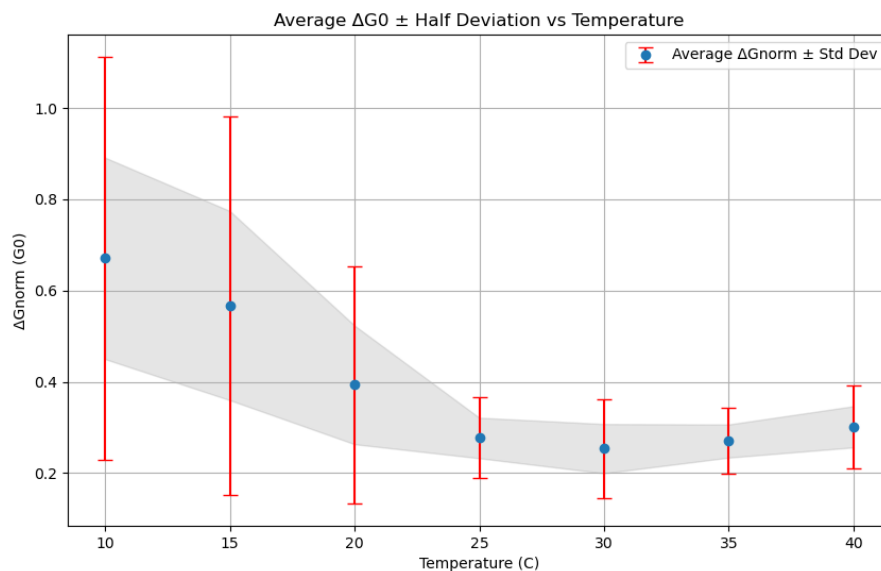


Figure 5.13: Average ΔG_0 vs Temperature

As reported in Figure 5.13, it is observed that ΔG_0 generally decreased as the temperature increased from 10°C to 30°C. Interestingly, there was a slight uptick at 40°C which was the maximum value for temperature in this experiment. Based on previous topics discussed in this work, there would be multiple explanations for seeing a minimum at 30 C. The balance between Ag^+ ions mobility and the thermal stability of the PVP matrix might result in a network configuration that is less prone to forming new conductive pathways. This stabilization could lead to the observed minimum in ΔG_0 . There could be effects against each other, while increasing temperature generally increases ion mobility leading to more significant changes in conductance, the network might also reach a point of stability at 30 C, where these effects balance out and could cause observed minimum.

5.4 Relative humidity effects on new sample with high G

Since sample 171N showed promising results with a small voltage pulse applied compared to 172N, we also decided to see the Relative Humidity effects on this sample. Instead of a 7V pulse voltage nanowire chip could show very good potentiation already at 0.5V. At constant ideal room temperature, one cycle (80-20-80%) of relative humidity was conducted. Since it is not several cycles we can not make any statistical outcome. It is observable from Figure 5.14 that, the average value of the conductance reaches its highest value when Relative humidity is also at max value for this experiment.

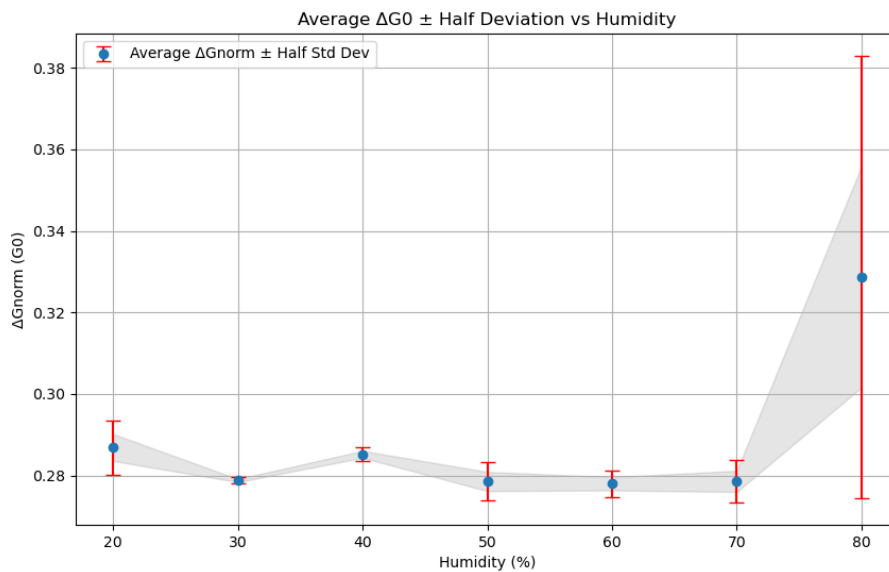


Figure 5.14: Average ΔG_0 vs Relative Humidity

Going through these measurements, one can realise how crucial it is to consider both the environmental conditions and the history of the material when interpreting the behaviour of nanowire networks. The results reveal the complexities involved and highlight the importance of maintaining consistency in experimental conditions to draw meaningful conclusions.

Chapter 6

Conclusion

Promising results from the study of neural networks and reservoir computing, especially with nanowires as hardware components for artificial intelligence, are increasingly being recognized. The goal of this thesis was to explore under which ideal conditions the dynamics of these neural networks would perform optimally for specific tasks. Given that the primary function of such reservoirs is their non-linear behaviour, the methods for fine-tuning these systems are complex and present numerous limitations and challenges.

The focus of this thesis is divided on studying the performance of Ag-PVP NWNs under two key environmental conditions: temperature and relative humidity.

Temperature, though it may seem a straightforward factor, has profound effects on the ability of neural networks to respond to input signals. The results at 5.3 showed that temperature variations lead to obvious changes in the conductance, higher temperatures were observed leading to a decrease in conductance. Results also highlight that repeated exposure to this temperature cycles, the nanowire network might be adapting in a way that leads to smaller changes in conductance.

The same questions were applied to relative humidity. In these conditions, the behaviour of Ag-PVP nanowires was found to be even more unstable. This instability is largely due to the significant role of electrochemical effects, which impact the nanowires' performance under varying humidity levels. In section 5.2, the data demonstrated a consistent increase in the average ΔG_0 with rising humidity levels. This trend is a possible result of enhanced redox activity and increased ionic mobility caused by the presence of water molecules which could act as a medium for silver ion migration.

This study validates the importance of environmental variables on the performance of Ag-PVP nanowires and also highlights theoretical background and future nanowire applications, particularly in reservoir computing and recurrent neural networks, which are central to large language models and other trending challenges.

Future research on the same topic could be done with the help of new and more precise experimental settings, incorporating computational simulations which could significantly improve understanding performance of nanowire networks.

Bibliography

Filipp Akopyan, Jun Sawada, Andrew Cassidy, Rodrigo Alvarez-Icaza, John Arthur, Paul Merolla, Nabil Imam, Yutaka Nakamura, Pallab Datta, Gi-Joon Nam, Brian Taba, Michael Beakes, Bernard Brezzo, Jente B. Kuang, Rajit Manohar, William P. Risk, Bryan Jackson, and Dharmendra S. Modha. Truenorth: Design and tool flow of a 65 mw 1 million neuron programmable neurosynaptic chip. *IEEE Transactions on Computer-Aided Design of Integrated Circuits and Systems*, 34(10):1537–1557, 2015. doi: 10.1109/TCAD.2015.2474396.

Samuel Aldana, Pedro García Fernández, Rocío Romero-Zaliz, Mireia Gonzalez, F. Jiménez-Molinos, Francesca Campabadal, F. Gómez-Campos, and Juan Roldan. A kinetic monte carlo simulator to characterize resistive switching and charge conduction in ni/hfo2/si rrams. pages 1–4, 11 2018. doi: 10.1109/CDE.2018.8597010.

Samuel Aldana, Pedro García Fernández, Rocío Romero-Zaliz, Mireia Gonzalez, F. Jiménez-Molinos, F. Gómez-Campos, Francesca Campabadal, and Juan Roldan. Resistive switching in hfo2 based valence change memories, a comprehensive 3d kinetic monte carlo approach. *Journal of Physics D: Applied Physics*, 53, 04 2020. doi: 10.1088/1361-6463/ab7bb6.

L. Appeltant, M. C. Soriano, G. Van der Sande, J. Danckaert, S. Massar, J. Dambre, B. Schrauwen, C. R. Mirasso, and I. Fischer. Information processing using a single dynamical node as complex system. *Nature Communications*, 2(1):468, 2011.

Tabassom Arjmand et al. Functional devices from bottom-up silicon nanowires: A review. *Nanomaterials*, 12(7):1043, 2022. doi: 10.3390/nano12071043.

Madeha Ahmed Awad, Eslam Mohamed Mohamed Ibrahim, and Ahmed Mohamed Ahmed. Synthesis and thermal stability of zno nanowires. *Journal of Thermal*

-
- Analysis and Calorimetry*, 117(2):635–642, 2014. ISSN 1588-2926. doi: 10.1007/s10973-014-3836-x. URL <https://doi.org/10.1007/s10973-014-3836-x>.
- Jun Bao, Jie-Xin Wang, Xiaofei Zeng, Liangliang Zhang, and J. Chen. Large-scale synthesis of uniform silver nanowires by high-gravity technology for flexible transparent conductive electrodes. *Industrial Engineering Chemistry Research*, 2019, 10 2019. doi: 10.1021/acs.iecr.9b04539.
- Y. Bengio, Patrice Simard, and Paolo Frasconi. Learning long-term dependencies with gradient descent is difficult. *IEEE transactions on neural networks / a publication of the IEEE Neural Networks Council*, 5:157–66, 02 1994. doi: 10.1109/72.279181.
- Dante R. Chialvo. Emergent complex neural dynamics. *Nature Physics*, 6(10):744–750, October 2010. ISSN 1745-2481. doi: 10.1038/nphys1803. URL <http://dx.doi.org/10.1038/nphys1803>.
- Kyunghyun Cho, Bart Merriënboer, Dzmitry Bahdanau, and Y. Bengio. On the properties of neural machine translation: Encoder-decoder approaches. 09 2014a. doi: 10.3115/v1/W14-4012.
- Kyunghyun Cho, Bart Merriënboer, Caglar Gulcehre, Fethi Bougares, Holger Schwenk, and Y. Bengio. Learning phrase representations using rnn encoder-decoder for statistical machine translation. 06 2014b. doi: 10.3115/v1/D14-1179.
- L. O. Chua. Memristor - the missing circuit element. *IEEE Transactions on Circuit Theory*, 18(5):507–519, 1971. doi: 10.1109/TCT.1971.1083337.
- Adrian Diaz Alvarez, Rintaro Higuchi, Paula Sanz-Leon, Ido Marcus, Yoshitaka Shingaya, Adam Stieg, James Gimzewski, Zdenka Kuncic, and Tomonobu Nakayama. Emergent dynamics of neuromorphic nanowire networks. *Scientific Reports*, 9, 10 2019a. doi: 10.1038/s41598-019-51330-6.
- Adrian Diaz Alvarez, Rintaro Higuchi, Paula Sanz-Leon, Ido Marcus, Yoshitaka Shingaya, Adam Stieg, James Gimzewski, Zdenka Kuncic, and Tomonobu Nakayama. Emergent dynamics of neuromorphic nanowire networks. *Scientific Reports*, 9, 10 2019b. doi: 10.1038/s41598-019-51330-6.
- Adrian Diaz Alvarez, Rintaro Higuchi, Paula Sanz-Leon, Ido Marcus, Yoshitaka Shingaya, Adam Stieg, James Gimzewski, Zdenka Kuncic, and Tomonobu Nakayama.

-
- Emergent dynamics of neuromorphic nanowire networks. *Scientific Reports*, 9, 10 2019c. doi: 10.1038/s41598-019-51330-6.
- Jeffrey L. Elman. Finding structure in time. *Cognitive Science*, 14(2):179–211, 1990. ISSN 0364-0213. doi: [https://doi.org/10.1016/0364-0213\(90\)90002-E](https://doi.org/10.1016/0364-0213(90)90002-E). URL <https://www.sciencedirect.com/science/article/pii/036402139090002E>.
- A. Erol, S. Okur, N. Yağmurcukardeş, and M.Ç. Arıkan. Humidity-sensing properties of a zno nanowire film as measured with a qcm. *Sensors and Actuators B: Chemical*, 152(1):115–120, 2011. ISSN 0925-4005. doi: <https://doi.org/10.1016/j.snb.2010.09.005>. URL <https://www.sciencedirect.com/science/article/pii/S0925400510007240>.
- Igor Farka, Radomír Bosák, and Peter Gergel. Computational analysis of memory capacity in echo state networks. *Neural networks : the official journal of the International Neural Network Society*, 83:109–120, 2016. URL <https://api.semanticscholar.org/CorpusID:8620735>.
- J. Fernandes, J. Grzonka, G. Araújo, A. Schulman, V. Silva, J. Rodrigues, J. Santos, O. Bondarchuk, P. Ferreira, P. Alpuim, and A. Capasso. Bipolar resistive switching in 2d mose₂ grown by atmospheric pressure chemical vapor deposition. *ACS Applied Materials & Interfaces*, 16(1):1767–1778, Jan 2024. doi: 10.1021/acsami.3c14215. Epub 2023 Dec 19, PMID: 38113456.
- Jun Ge and Mohamed Chaker. Oxygen vacancies control transition of resistive switching mode in single-crystal tio₂ memory device. *ACS Applied Materials & Interfaces*, 9(19):16327–16334, May 2017. ISSN 1944-8244. doi: 10.1021/acsami.7b03527. URL <https://doi.org/10.1021/acsami.7b03527>.
- Felix Gers, Jürgen Schmidhuber, and Fred Cummins. Learning to forget: Continual prediction with lstm. *Neural computation*, 12:2451–71, 10 2000. doi: 10.1162/089976600300015015.
- Alex Graves. Generating sequences with recurrent neural networks. 08 2013.
- Davide Grazioli, Gabriele Gangi, Lucia Nicola, and Angelo Simone. Predicting mechanical and electrical failure of nanowire networks in flexible transparent electrodes. *Composites Science and Technology*, 245:110304, 2024. ISSN 0266-3538. doi: <https://doi.org/10.1016/j.compscitech.2024.110304>.

//doi.org/10.1016/j.compscitech.2023.110304. URL <https://www.sciencedirect.com/science/article/pii/S0266353823003986>.

Xinyu Han, Yi Zhao, and Michael Small. Revisiting the memory capacity in reservoir computing of directed acyclic network. *Chaos: An Interdisciplinary Journal of Nonlinear Science*, 31:033106, 03 2021. doi: 10.1063/5.0040251.

Jeffrey Heaton. Ian goodfellow, yoshua bengio, and aaron courville: Deep learning: The mit press, 2016, 800 pp, isbn: 0262035618. *Genetic Programming and Evolvable Machines*, 19, 10 2017. doi: 10.1007/s10710-017-9314-z.

Sepp Hochreiter and Jürgen Schmidhuber. Long short-term memory. *Neural computation*, 9:1735–80, 12 1997. doi: 10.1162/neco.1997.9.8.1735.

Chenghao Hu and Baochun Li. Distributed inference with deep learning models across heterogeneous edge devices. In *IEEE INFOCOM 2022 - IEEE Conference on Computer Communications*, pages 330–339. IEEE, 2022.

Liangbing Hu, Han Kim, Jung-Yong Lee, Peter Peumans, and Yi Cui. Scalable coating and properties of transparent, flexible, silver nanowire electrodes. *ACS nano*, 4:2955–63, 05 2010. doi: 10.1021/nn1005232.

Keithley Instruments. The simple choice for complex characterization tasks: Model 4200-scs semiconductor characterization system. 2018. URL <https://www.imperial.ac.uk/media/imperial-college/research-centres-and-groups/centre-for-bio-inspired-technology/7291000.PDF>. Accessed: [7th May 2024].

Herbert Jaeger. Short term memory in echo state networks. 01 2002.

Kim Jongmin, Kyoocho Jung, Yongmin Kim, Yongcheol Jo, Sangeun Cho, Hyeonseok Woo, Seongwoo Lee, A Inamdar, Jinpyo Hong, Jeon-Kook Lee, and Hyunsik Im. Switching power universality in unipolar resistive switching memories. *Scientific reports*, 6:23930, 04 2016. doi: 10.1038/srep23930.

Franklin Kim, Serena Kwan, Jennifer Akana, and Peidong Yang. Langmuir–blodgett nanorod assembly. *Journal of the American Chemical Society*, 123:4360–1, 06 2001. doi: 10.1021/ja0059138.

-
- Pengfei Kou, Liu Yang, Cheng Chang, and Sailing He. Improved flexible transparent conductive electrodes based on silver nanowire networks by a simple sunlight illumination approach. *Scientific Reports*, 7(1):42052, Feb 2017. doi: 10.1038/srep42052. URL <https://doi.org/10.1038/srep42052>.
- Qin Kuang, Changshi Lao, Zhong Lin Wang, Zhaoxiong Xie, and Lansun Zheng. High-sensitivity humidity sensor based on a single SnO_2 nanowire. *State Key Laboratory for Physical Chemistry of Solid Surfaces Department of Chemistry, Xiamen University, Xiamen 361005, China, and School of Materials Science and Engineering, Georgia Institute of Technology, Atlanta, Georgia 30332-0245*, 2007. Received February 3, 2007.
- Ankur Kumar, Mukesh Kumar, M.S. Goyat, and D.K. Avasthi. A review of the latest developments in the production and applications of ag-nanowires as transparent electrodes. *Materials Today Communications*, 33:104433, 2022. ISSN 2352-4928. doi: <https://doi.org/10.1016/j.mtcomm.2022.104433>. URL <https://www.sciencedirect.com/science/article/pii/S2352492822012740>.
- Zdenka Kuncic and Tomonobu Nakayama. Neuromorphic nanowire networks: principles, progress and future prospects for neuro-inspired information processing. *Advances in Physics: X*, 6(1):1894234, 2021. doi: 10.1080/23746149.2021.1894234. URL <https://doi.org/10.1080/23746149.2021.1894234>.
- S.T. Lee, N. Wang, and C.S. Lee. Semiconductor nanowires: synthesis, structure and properties. *Materials Science and Engineering: A*, 286(1):16–23, 2000. ISSN 0921-5093. doi: [https://doi.org/10.1016/S0921-5093\(00\)00658-4](https://doi.org/10.1016/S0921-5093(00)00658-4). URL <https://www.sciencedirect.com/science/article/pii/S0921509300006584>.
- Rui Liu, Gang Qiu, Bing Chen, Gao Bin, and Jinfeng Kang. Degradation characteristics of resistive switching memory devices correlated with electric field induced ion-migration effect of anode. *Chinese Physics Letters*, 30, 11 2013. doi: 10.1088/0256-307X/30/11/117104.
- Yun-Ze Long, Miao Yu, Bin Sun, Chang-Zhi Gu, and Zhiyong Fan. Recent advances in large-scale assembly of semiconducting inorganic nanowires and nanofibers for electronics, sensors and photovoltaics. *Chem. Soc. Rev.*, 41:4560–4580, 2012. doi: 10.1039/C2CS15335A. URL <http://dx.doi.org/10.1039/C2CS15335A>.

-
- Yoochan Ma, Geon Woo Sim, Sungjin Jo, Dong Choon Hyun, Jae-Seung Roh, Dongwook Ko, and Jongbok Kim. Stability of silver-nanowire-based flexible transparent electrodes under mechanical stress. *Applied Sciences*, 14(1), 2024. ISSN 2076-3417. doi: 10.3390/app14010420. URL <https://www.mdpi.com/2076-3417/14/1/420>.
- Hugh Manning, Fabio Niosi, Claudia Gomes da Rocha, Allen Bellew, Colin O’Callaghan, Subhajit Biswas, Patrick Flowers, Ben Wiley, Justin Holmes, Mauro Ferreira, and John Boland. Emergence of winner-takes-all connectivity paths in random nanowire networks. 04 2018.
- Carver Mead. Neuromorphic electronic systems. *Proceedings of the IEEE*, 78(10): 1629–1636, 1990.
- MicroprobeSystems. Custom temperature and humidity chamber information, 2024a. URL https://microprobesystem.com/chamber.html#custom_Thum. Accessed: [1st August 2024].
- MicroprobeSystems. Humidity controller information, 2024b. URL <https://microprobesystem.com/controller.html#humidity>. Accessed: [1st August 2024].
- Gianluca Milano, Giacomo Pedretti, M. Fretto, Luca Boarino, Fabio Benfenati, D. Ielmini, Ilia Valov, and Carlo Ricciardi. Brain-inspired structural plasticity through reweighting and rewiring in multi-terminal self-organizing memristive nanowire networks. *Advanced Intelligent Systems*, 2, 06 2020a. doi: 10.1002/aisy.202000096.
- Gianluca Milano, Federico Raffone, Michael Luebben, Luca Boarino, Giancarlo Cicero, Ilia Valov, and Carlo Ricciardi. Water-mediated ionic migration in memristive nanowires with a tunable resistive switching mechanism. *ACS Applied Materials & Interfaces*, 12(43):48773–48780, 2020b. doi: 10.1021/acsami.0c13020. URL <https://doi.org/10.1021/acsami.0c13020>. PMID: 33052645.
- Gianluca Milano, Michael Lübben, Marco Laurenti, Luca Boarino, Carlo Ricciardi, and Ilia Valov. Structure-dependent influence of moisture on resistive switching behavior of zno thin films. *Advanced Materials Interfaces*, 8, 07 2021. doi: 10.1002/admi.202100915.

-
- Gianluca Milano, Giacomo Pedretti, Kevin Montano, Saverio Ricci, Shahin Hashemkhani, Luca Boarino, D. Ielmini, and Carlo Ricciardi. In materia reservoir computing with a fully memristive architecture based on self-organizing nanowire networks. *Nature Materials*, 21:1–8, 02 2022. doi: 10.1038/s41563-021-01099-9.
- Kevin Montano, Gianluca Milano, and Carlo Ricciardi. Grid-graph modeling of emergent neuromorphic dynamics and heterosynaptic plasticity in memristive nanonetworks. *Neuromorphic Computing and Engineering*, 2, 02 2022. doi: 10.1088/2634-4386/ac4d86.
- Nicolas Onofrio, David Guzman, and Alejandro Strachan. Atomic origin of ultrafast resistance switching in nanoscale electrometallization cells. *Nature materials*, 14, 03 2015. doi: 10.1038/nmat4221.
- Jey Panisilvam, Ha Young Lee, Sujeong Byun, Daniel Fan, and Sejeong Kim. Two-dimensional material-based memristive devices for alternative computing. *Nano Convergence*, 11(1):25, Jun 2024. doi: 10.1186/s40580-024-00432-7. URL <https://doi.org/10.1186/s40580-024-00432-7>.
- Razvan Pascanu, Tomas Mikolov, and Y. Bengio. On the difficulty of training recurrent neural networks. *30th International Conference on Machine Learning, ICML 2013*, 11 2012.
- R. K. Pathria and Paul D. Beale. *Statistical Mechanics*. Elsevier, Amsterdam, Netherlands, 3rd edition, 2011.
- Shubham Patil, N.B. Mullani, Kiran Nirmal, Gihwan Hyun, Batyrbek Alimkhanuly, Rajanish Kamat, Jun Park, Sanghoek Kim, and Dr. T. Dongale. Spike-time dependent plasticity of tailored zno nanorod-based resistive memory for synaptic learning. *Journal of Science: Advanced Materials and Devices*, 8:100617, 08 2023. doi: 10.1016/j.jsamd.2023.100617.
- D. P. Pattnaik, C. Andrews, M. D. Cropper, A. Gabbitas, A. G. Balanov, S. Savel'ev, and P. Borisov. Gamma radiation-induced nanodefects in diffusive memristors and artificial neurons. *Nanoscale*, 15:15665–15674, 2023. doi: 10.1039/D3NR01853A. URL <https://doi.org/10.1039/D3NR01853A>. Received 21st April 2023, Accepted 20th August 2023, First published on 31st August 2023.

- Ajeng Prameswati, Joo Won Han, Jung Ha Kim, Anky Fitriani Wibowo, Siti Aisyah Nurmaulia Entifar, Jihyun Park, Jonghee Lee, Soyeon Kim, Dong Chan Lim, Myoung-Woon Moon, Min-Seok Kim, and Yong Hyun Kim. Highly stretchable and mechanically robust silver nanowires on surface-functionalized wavy elastomers for wearable healthcare electronics. *Organic Electronics*, 108:106584, 2022. ISSN 1566-1199. doi: <https://doi.org/10.1016/j.orgel.2022.106584>. URL <https://www.sciencedirect.com/science/article/pii/S1566119922001562>.
- S. Raoux, G. W. Burr, M. J. Breitwisch, C. T. Rettner, Y.-C. Chen, R. M. Shelby, M. Salinga, D. Krebs, S.-H. Chen, H.-L. Lung, and C. H. Lam. Phase-change random access memory: A scalable technology. *IBM Journal of Research and Development*, 52(4.5):465–479, 2008. doi: 10.1147/rd.524.0465.
- Luis Reinaudi, Christian F.A. Negre, and M. Cecilia Gimenez. Monte carlo simulations for understanding the transport properties of metallic nanowires. *Physica E: Low-dimensional Systems and Nanostructures*, 124:114326, 2020. ISSN 1386-9477. doi: <https://doi.org/10.1016/j.physe.2020.114326>. URL <https://www.sciencedirect.com/science/article/pii/S1386947720305737>.
- Kaushik Roy, Akhilesh Jaiswal, and Priyadarshini Panda. Beyond von-neumann computing with emerging memory technologies. *Nature Electronics*, 2(5):252–253, 2019.
- Billel Salhi. Nanowires: Synthesis, applications and challenges. *Journal of Biomedical Research Studies*, 1(3), Dec 2020. doi: 10.32474/JBRS.2020.01.000112. URL <https://doi.org/10.32474/JBRS.2020.01.000112>. Received: October 12, 2020; Published: December 09, 2020.
- Lauri Salmela, Nikolaos Tsipinakis, Alessandro Foi, Cyril Billet, John Dudley, and G. Genty. Predicting ultrafast nonlinear dynamics in fibre optics with a recurrent neural network. *Nature Machine Intelligence*, 3:1–11, 04 2021. doi: 10.1038/s42256-021-00297-z.
- Akihito Sawa. Resistive switching in transition metal oxides. *Materials Today*, 11(6):28–36, 2008. ISSN 1369-7021. doi: [https://doi.org/10.1016/S1369-7021\(08\)70119-6](https://doi.org/10.1016/S1369-7021(08)70119-6). URL <https://www.sciencedirect.com/science/article/pii/S1369702108701196>.

-
- Benjamin Schrauwen, David Verstraeten, and Jan Campenhout. An overview of reservoir computing: Theory, applications and implementations. pages 471–482, 2007.
- Fairuz Septiningrum, Liszulfah Roza, and Vivi Fauzia. The effect of temperature and reaction time on the shape of ag nanowires synthesized using the polyol method. *IOP Conference Series: Materials Science and Engineering*, 622(1):012031, oct 2019. doi: 10.1088/1757-899X/622/1/012031. URL <https://dx.doi.org/10.1088/1757-899X/622/1/012031>.
- Huang Sheng-Yun, Qingzhe Zhang, Fan Yang, Deepak Thrithamarassery Gangadharan, Pandeng Li, Fuqiang Ren, Baoquan Sun, and Dongling Ma. A facile way for scalable fabrication of silver nanowire network electrodes for high-performance and foldable smart windows. *Journal of Materials Chemistry A*, 8, 04 2020. doi: 10.1039/C9TA14030A.
- Manseong Song and Su-Chul Yang. Investigation of ferromagnetic and ferroelectric properties in binderless cellulose/ni laminates for magnetoelectric applications. *Polymers*, 14:5347, 12 2022. doi: 10.3390/polym14245347.
- Ilya Sutskever, Oriol Vinyals, and Quoc Le. Sequence to sequence learning with neural networks. *Advances in Neural Information Processing Systems*, 4, 09 2014.
- Y. Y. Tarasevich, I. V. Vodolazskaya, and A. V. Eserkepov. Electrical conductivity of random metallic nanowire networks: An analytical consideration along with computer simulation. *ArXiv*, 2022. doi: 10.1039/D2CP00936F. URL <https://doi.org/10.1039/D2CP00936F>.
- Katsuhiko Terabe, Tsuyoshi Hasegawa, Tomonori Nakayama, and Masakazu Aono. Quantized conductance atomic switch. *Nature*, 433(7021):47–50, 2005.
- A. Wagner and H. Kliem. Monte-carlo simulation of three dimensional ion dynamics in polymers. *MRS Online Proceedings Library*, 653(1):10101, 2011. doi: 10.1557/PROC-653-Z10.10. URL <https://doi.org/10.1557/PROC-653-Z10.10>.
- S. Wang, Z. Shan, and H. Huang. The mechanical properties of nanowires. *Advanced Science (Weinheim)*, 4(4):1600332, 2017. doi: 10.1002/advs.201600332. URL <https://doi.org/10.1002/advs.201600332>. Published 2017 Jan 3.

-
- R. Waser, R. Dittmann, G. Staikov, and K. Szot. Redox-based resistive switching memories - nanoionic mechanisms, prospects, and challenges. *Advanced Materials*, 21(25-26):2632–2663, 2009. doi: 10.1002/adma.200900375. URL <https://doi.org/10.1002/adma.200900375>.
- Rainer Waser and Masakazu Aono. Nanoionics-based resistive switching memories. *Nature Materials*, 6(11):833–840, Nov 2007. ISSN 1476-4660. doi: 10.1038/nmat2023. URL <https://doi.org/10.1038/nmat2023>.
- Rainer Waser, Regina Dittmann, Stephan Menzel, and Tobias Noll. Introduction to new memory paradigms: Memristive phenomena and neuromorphic applications. *Faraday Discussions*, 213, 02 2019. doi: 10.1039/C8FD90058B.
- S. A. Wolf, D. D. Awschalom, R. A. Buhrman, J. M. Daughton, S. von Molnár, M. L. Roukes, A. Y. Chtchelkanova, and D. M. Treger. Spintronics: a spin-based electronics vision for the future. *Science*, 294(5546):1488–1495, Nov 2001. doi: 10.1126/science.1065389.
- Qixuan Xiang, Rahul Navik, Huijun Tan, and Yaping Zhao. Synthesis of oxidation-resistance copper nanowires-formate for high-performance transparent conductive electrodes. *Journal of Alloys and Compounds*, 914:165265, 2022. ISSN 0925-8388. doi: <https://doi.org/10.1016/j.jallcom.2022.165265>. URL <https://www.sciencedirect.com/science/article/pii/S0925838822016565>.
- Wuhong Xue, Shuang Gao, Jie Shang, Xiaohui Yi, Gang Liu, and Run-Wei Li. Recent advances of quantum conductance in memristors. *Advanced Electronic Materials*, 5: 1800854, 02 2019a. doi: 10.1002/aelm.201800854.
- Wuhong Xue, Shuang Gao, Jie Shang, Xiaohui Yi, Gang Liu, and Run-Wei Li. Recent advances of quantum conductance in memristors. *Advanced Electronic Materials*, 5: 1800854, 02 2019b. doi: 10.1002/aelm.201800854.
- J. J. Yang, D. B. Strukov, and D. R. Stewart. Memristive devices for computing. *Nature Nanotechnology*, 8(1):13–24, 2013. doi: 10.1038/nnano.2012.240. URL <https://doi.org/10.1038/nnano.2012.240>.
- Yusheng Yang, Bai Sun, Zelin Cao, Shuangso Mao, Jiajia Qin, Zhaowei Rao, Mingnan Liu, Chuan Ke, and Yong Zhao. Moisture-modulated resistive switching be-


havior based on cati₃ prepared by the appropriate naoh concentration. *Chemical Physics*, 578:112161, 2024. ISSN 0301-0104. doi: <https://doi.org/10.1016/j.chemphys.2023.112161>. URL <https://www.sciencedirect.com/science/article/pii/S0301010423003439>.

Xiaohan Zhang, Xiaoning Zhao, Xuanyu Shan, Qiaoling Tian, Zhongqiang Wang, Ya Lin, Xu Haiyang, and Y. Liu. Humidity effect on resistive switching characteristics of the ch₃nh₃pbi₃ memristor. *ACS Applied Materials Interfaces*, 13, 06 2021. doi: 10.1021/acsami.1c05590.

Yangyang Zhang, Manoj K. Ram, Elias K. Stefanakos, and D. Yogi Goswami. Synthesis, characterization, and applications of zno nanowires. *Journal of Nanomaterials*, 2012: 624520, 2012. doi: 10.1155/2012/624520. URL <https://doi.org/10.1155/2012/624520>. First published: 17 July 2012.

Statement of Non-Plagiarism

I hereby declare that all information in this report has been obtained and presented in accordance with academic rules and ethical conduct and the work I am submitting in this report, except where I have indicated, is my own work.

Signature: 

Date: 26 August 2024

Supervisor Approval

I, the undersigned, Prof. Carlo Ricciardi, supervisor of Khayal Azizli, student of the EMJMD Photonics for Security Reliability and Safety, during his master thesis at the Polytechnic University of Turin certify that I approve the content of this master thesis report entitled 'Impact of humidity and temperature on nanowire networks dynamics'.


Name: Prof. Carlo Ricciardi

Signature: 

Date: 26 August 2024

Copyright of Figures

All figures and illustrations in this thesis are either my creations/drawn or have been adapted/collected from academic journals. Proper credit has been given in the figure captions where required.

Signature: 

Date: 26 August 2024